JPG Journal of Petroleum Geology www.jpg.co.uk

Journal of Petroleum Geology, Vol. 45(2), April 2022, pp 179-200

TECTONOSTRATIGRAPHIC EVOLUTION AND HYDROCARBON PROSPECTIVITY SOUTH OF GWADAR BAY, MAKRAN ACCRETIONARY WEDGE, OFFSHORE SW PAKISTAN

Conall Cromie[1,2]*, Nicola Scarselli[1], Jonathan Craig[1,3], Moin R. Khan[4] and Abid Hussain[4]

The Makran accretionary wedge developed as a result of subduction of the Arabian Plate beneath the southern margin of Eurasia since the Eocene. Interpretation of 2D seismic profiles calibrated to offshore well data in a study area to the south of Gwadar Bay (SW Pakistan) indicates a major period of accretion from the mid-Miocene, as evidenced by the occurrence of thick growth strata associated with large-scale imbricate thrusts. The thrust faults originate from a deep detachment within the mud-rich Oligocene interval, and well-developed piggy-back basin successions occur in thrust hanging walls. In the study area, the thrust structures are sealed by a thick, progradational Pliocene to Recent interval in which the presence of submarine canyons, up to 2.5 km across, indicate that sedimentary transport was from the north.

Fluid escape pipes and associated amplitude anomalies are observed in the seismic profiles studied and may be related to upward migration of thermogenic hydrocarbons from depth, as heavy hydrocarbon fractions >C_3 have been reported from nearby wells. The hydrocarbons are believed to have been sourced from the Oligocene Hoshab Shale and to have then migrated up through a sedimentary succession in which permeability barriers are largely absent. Hanging wall anticlines mapped in the study area could provide structural traps, and turbidites in the Lower Miocene Panjgur Formation may represent a potential reservoir. Amplitude anomalies are also observed adjacent to shallow fluid escape pipes within the topsets of clinoforms in the Pleistocene Chatti and Omara Formations, and probably indicate the presence of biogenic hydrocarbons sourced from distal mudstones in bottomset strata.

[1] Earth Science Department, Royal Holloway University of London, Egham Hill, Egham, TW20 0EX.
[2] RPS Group, Goldvale House, Church Street West, Woking GU21 6DH.
[3] Eni Natural Resources, Via Emilia 1, 20097 San Donato Milanese, Milan, Italy.
[4] Pakistan Petroleum Limited, 4th Floor, PIDC House, Karachi 75530, Pakistan.

*Corresponding author, email:
conallcromie98@gmail.com

Key words: Pakistan, offshore, Makran accretionary wedge, fluid escape features, prospectivity, hydrocarbons, growth strata, amplitude anomalies, imbricate thrusts, seismic stratigraphy.

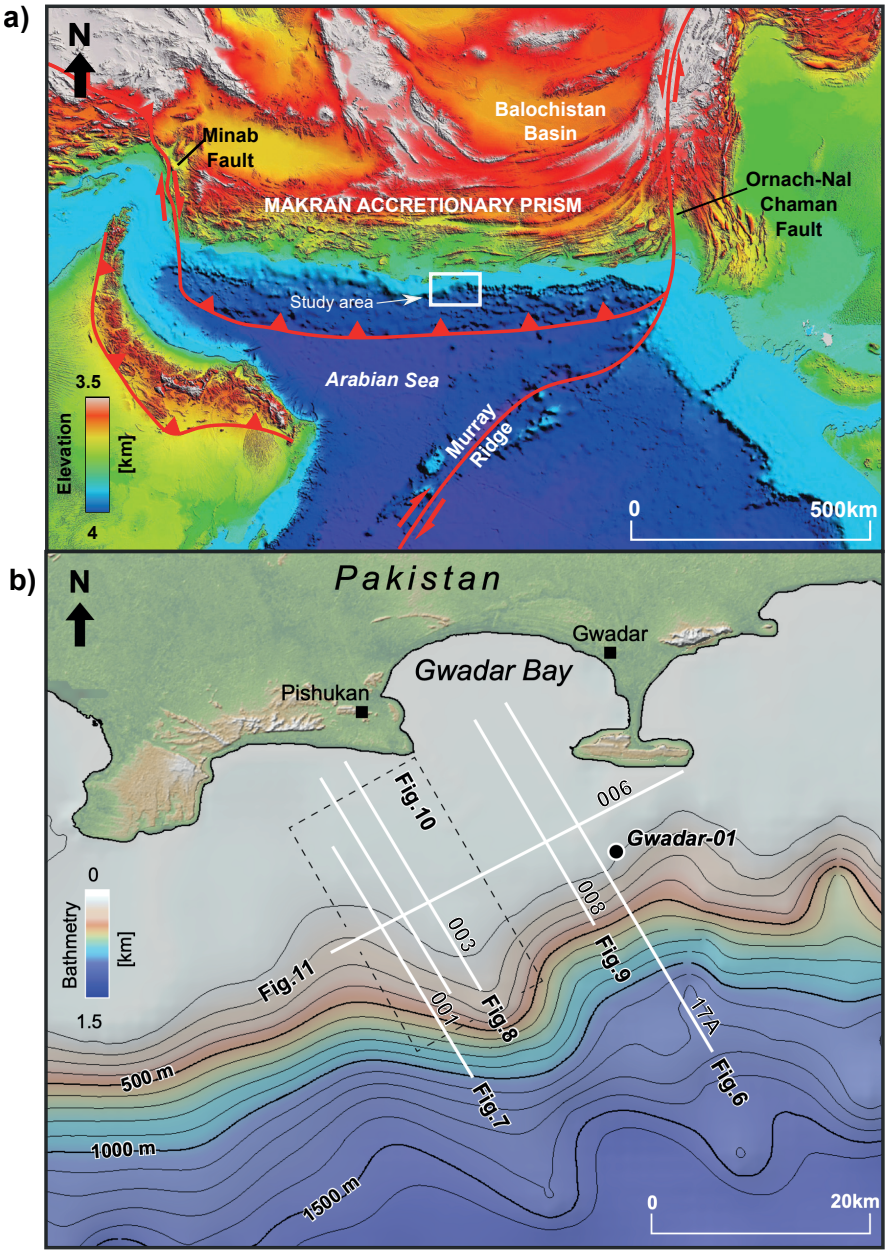

Fig. 1. (a) Digital Elevation Model (DEM) illustrating the main features of the Makran accretionary prism and the surrounding region. The study area offshore Gwadar Bay in SW Pakistan is marked by the box. (b) Bathymetric map of the study area showing the location of the Gwadar-01 well and the 2D seismic lines studied.

INTRODUCTION

The Makran accretionary wedge (or "Makran") extends east-west for about 1000 km along the Arabian Sea coast of southern Pakistan and Iran, with a deformation front located offshore about 150 km to the south of the coastline (Fig 1a). The Makran is the product of active subduction of the Arabian Plate beneath the southern Eurasia margin and is in general composed of a series of imbricate thrusts which have developed above a tectonically underplated sedimentary succession (Fig. 2) (Grando and McClay, 2007; Burg, 2018; Kopp *et al.*, 2000; Platt *et al.*, 1985; Ellouz-Zimmermann *et al.*, 2008; Smith *et al.*, 2012). Gas seeps and mud volcanoes are reported to occur both on- and offshore (Kassi *et al.*, 2014; Delisle, 2004; Delisle *et al.*, 2001; Grando and McClay, 2007; Schlüter *et al.*, 2002; Tabrez and Inam, 2012) and, together with fluid escape pipes and other fluid escape features observed in seismic profiles (Hussain *et al.*, 2015), suggest the possible presence of an active petroleum system. Fault propagation anticlines in the hanging walls of thrust faults constitute potential structural traps (Hussain *et al.*, 2015), although only very few wells have been drilled in the Makran region so far. This paper aims to improve understanding of the tectonostratigraphic evolution of the Makran accretionary wedge in an area located offshore Gwadar Bay (SW Pakistan) (Fig. 1b) and to

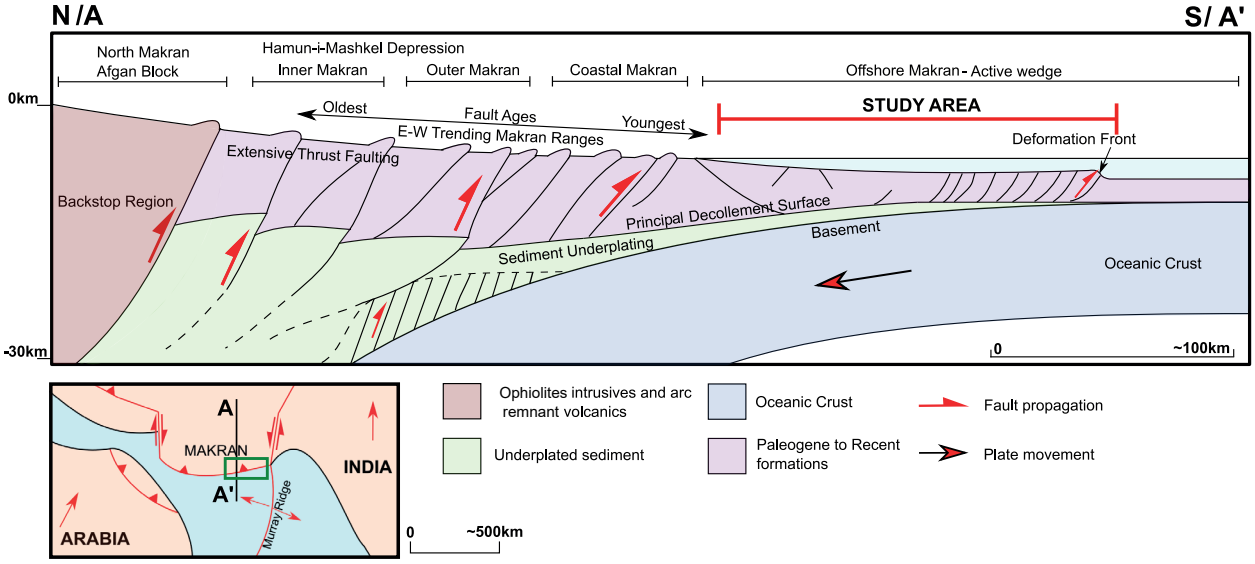

Fig. 2. Schematic section illustrating the generalised structure of the Makran accretionary prism (after Burg, 2018; Grando and McClay, 2007; Kopp *et al.*, 2000). The study area and the location of the section are shown in the inset map below.

assess the hydrocarbon potential of the region using 2D seismic profiles tied to the Gwadar 1 exploration well.

Geological setting

The Makran accretionary wedge formed as a result of northwards subduction of the Arabian Plate beneath the southern margin of the Eurasian Plate beginning in the Late Cretaceous. Shallow-angled subduction has occurred since the Oligocene (Kopp *et al.*, 2000) at a rate of approximately 4 cm yr^{-1}, varying from of 4.2 cm yr^{-1} in the east of the wedge to 3.65 cm yr^{-1} in the west (DeMets *et al.*, 2010). The accretionary wedge is bounded at its eastern and western flanks by north-south trending strike-slip fault zones (Safari *et al.*, 2017): the Ornach-Nal-Chaman fault in the east, and the Minab-Sabzevaran fault in the west (Fig. 1a) (White and Ross, 1979). The onshore Ornach-Nal-Chaman fault delineates the Indian Plate from the Balochistan Basin and is linked to the offshore Murray Ridge and Owen Fracture Zone (De Mets *et al.*, 1990).

Subduction of northern NeoTethys beneath the southern Eurasian margin began as early as 130 Ma (Burg, 2018) with the formation of magmatic arcs (e.g. the Bajan Durkan Complex). Development of an accretionary wedge in the Makran region began in the Eocene (Byrne *et al.*, 1992) at the same time as the final convergence and docking of India with Eurasia. A second major phase of imbrication in the Makran took place in the mid-Miocene (Platt, 1988) and was accompanied by the beginning of intense sediment underplating. Propagation of the wedge and further underplating took place in the Pliocene and continues at the present day (Schlüter *et al.*, 2002).

To the north of the Makran, a backstop region consists of ophiolites, intrusive rocks and arc-remnant volcanics of pre-Cretaceous age. Within the accretionary prism, thrust faults propagate southwards and the age of faulting has been determined by fission-track apatite ages which vary from 23 Ma to approximately 7.9 Ma (Dolati, 2010). Extension has been documented at the continental shelf (Grando and McClay., 2007) with imbricate thrusting taking place further south towards the offshore deformation front. The thrusts have been interpreted to sole out at a principal detachment surface (Schlüter *et al.*, 2002) within a turbidite megasequence which is Late Cretaceous to Paleogene in age.

Diapirism has been widely documented in the shelf region of the Makran (Grando and McClay., 2007; Schlüter *et al.*, 2002) and is interpreted to be related to the mud volcanoes and gas seeps which are recorded both on- and offshore. Mud volcanoes are found throughout the Makran in proximity to fault-related folds where breaching and fluid escape has occurred (Grando and McClay, 2007).

Stratigraphy and petroleum systems elements

The general stratigraphy in the Makran was first defined by Hunting Survey Corporation (1960) followed by Cheema *et al.* (1977), with later modifications by Critelli *et al.* (1990), Ellouz-Zimmerman *et al.* (2007) and Back and Morley (2016) (Fig. 3). These studies provide an overview of the lithologic characteristics of key formations in the region although uncertainties persist regarding the units' ages.

The sedimentary column is ~7 km thick and ranges in age from Cretaceous to Recent (Fig. 3) (Burg, 2018). Sedimentary rocks rest on Cretaceous or older basement which is composed of ophiolites, intrusives and arc-remnant volcanics, and which is exposed in the Hamun-e-Mashkel depression to the north of the Makran in Balochistan (SW Pakistan) where it

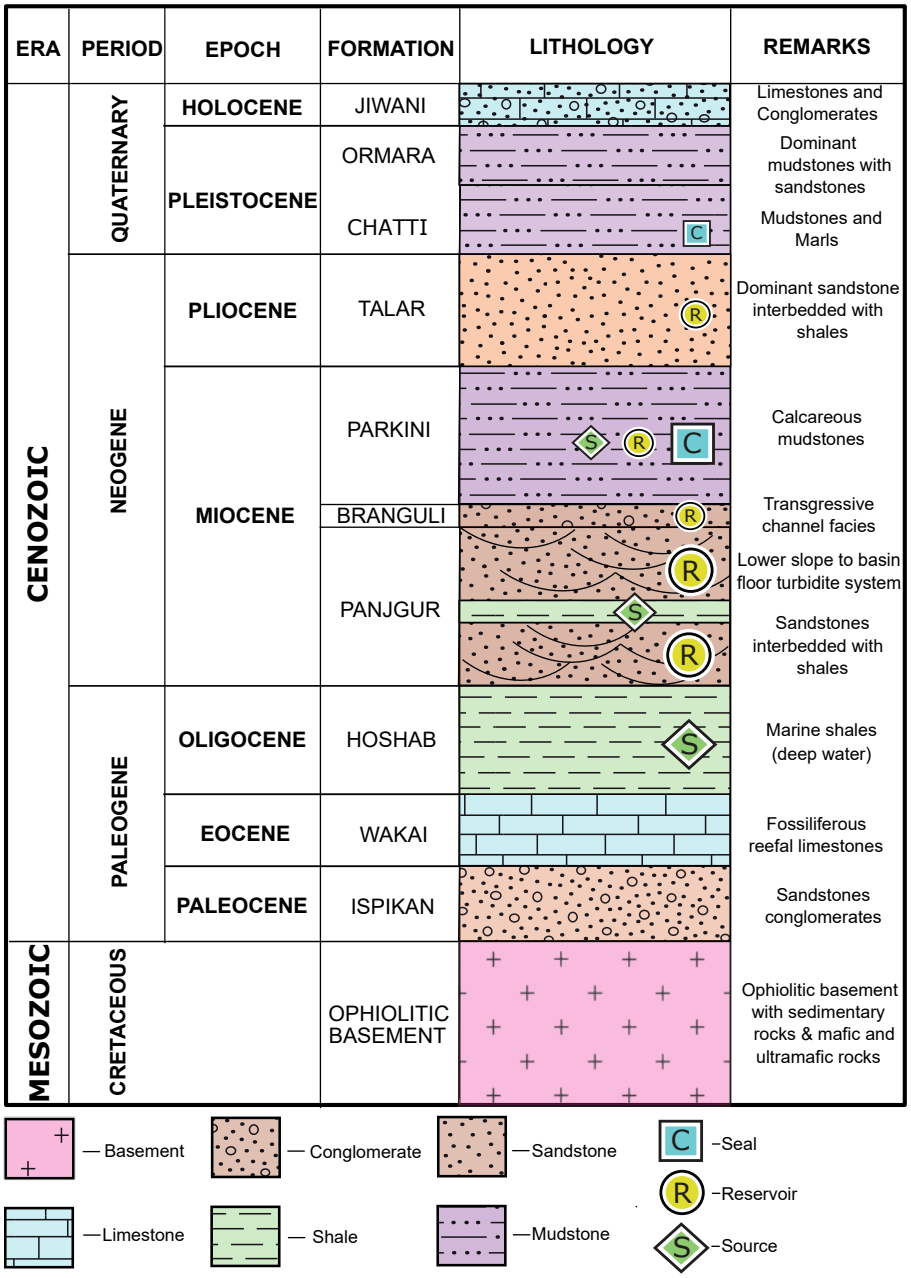

Fig. 3. Generalised stratigraphic chart for the Pakistani Makran (compiled from Ellouz-Zimmerman *et al.*, 2007; Hussain *et al.*, 201; Kahn and Clyde, 2013; and Back and Morley, 2016) with petroleum system elements.

constitutes a backstop for the accretionary prism. The bulk of the overlying sedimentary succession is interpreted to consist of detrital material derived from the uplifting and eroding Himalayas which was transported via the palaeo-Indus river system to the Arabian Sea (Grigsby *et al.*, 2009). At the base of the sedimentary column in the Pakistani Makran are the Paleocene sandstones, laminated mudstones and conglomerates of the Ispikan Formation which are overlain by the shallow water Eocene limestones of the Wakai Formation (Kassi *et al.*, 2007; Cheema *et al.*, 1977). The Oligocene Hoshab Formation consists of deep-marine shales and mudstones (Kassi *et al.*, 2011) which at outcrops onshore have TOC contents of up to 0.6% (Kahn *et al.*, 1991). The formation may also have a high organic content offshore (Gwadar Well Geological Report – Benrud *et al.*, 2000) and has been interpreted as a potential source rock (Hussain *et al.*, 2015).

The Lower Miocene Panjgur Formation consists of medium- to coarse-grained turbidite sandstones whose estimated thickness ranges from 450 m (Kassi *et al.*, 2011) to 2-3 km (Platt *et al.*, 1985). The sandstones are highly fractured and display excellent primary reservoir characteristics, with significant secondary porosity formed by calcite dissolution (Grigsby *et al.*, 2009), as do the thick sandstones in the mid-Miocene Branguli Formation (Critelli *et al.*, 1990).

The upper Miocene Parkini Formation is up to 3 km thick (Malkani, 2020) and consists of calcareous

Table 1. Table showing the formation tops at well Gwadar-01 (Operator: Ocean Pakistan Corporation), with the measured depths in metres and time in TWT (ms). The formation age at TD (3810 m) was early Tortonian (late Miocene).

Formation Tops	Measured Depth (m)	TWT (ms)
Holocene	374.9	410.8
Pleistocene	1033.2	992.7
Pliocene	1289.3	1266.1
Miocene	1371.6	1299.5

mudstones (Back and Morley, 2016) which may have both source rock and seal potential. TOC contents of 0.46-0.98% (Kahn *et al.*,1991) have been recorded in outcrops onshore. Sandstones in the upper part of the formation may have reservoir potential.

The overlying Talar Formation (Pliocene) consists of medium- to coarse-grained sandstones with minor mudstones and shales (Ahmed, 1968). Sandstone units are resistant to weathering and occur at the surface over large parts of the Makran (Hunting Survey Corporation, 1960; Ahmed, 1968; Back and Morley, 2016). They are overlain by fine-grained calcareous muds and marls of the lower Pleistocene Chatti Formation (Ellouz-Zimmerman *et al.*, 2007; Kassi *et al.*, 2007). The Ormara and Jiwani Formations (upper Pleistocene to Holocene) are dominated by mudstones with minor sandstones and shallow-water limestone and conglomerates respectively (Ahmed, 1968; Back and Morley, 2016).

In terms of petroleum systems elements (Fig. 3), potential source rocks comprise the Parkini and Hoshab Formations (Kahn *et al.*,1991, Hussain *et al.*, 2015). The lower Miocene Panjgur Formation has favourable reservoir characteristics (e.g. Grigsby *et al.*, 2009) in the onshore Makran and is the primary exploration target offshore. However, the lateral distribution of the Panjgur turbidite fans is not clear, nor is the formation's offshore extent. The overlying Parkini Formation mudstones could provide a top seal. Fault propagation folds in the hanging walls of thrust faults are widespread in the Makran and represent potential traps for hydrocarbons.

However, the on- and offshore Makran region has not been extensively studied and only nine wells have been drilled in the Makran in Pakistan (four offshore and five onshore), all of which were unsuccessful. The most recent exploration well (Pasni X-2) was drilled in 2005 by Pakistan Petroleum Limited (PPL) to a total depth of around 4000 m but did not reach the target Panjgur Formation reservoir sandstones. Likewise, relatively little information on oil and gas exploration is available for the Iranian Makran and no commercial discoveries in the offshore area have as yet been reported.

DATASET AND METHODS

The data available for this study consists of five 2D time-migrated seismic lines – 001, 003, 006, 008 and 17A – located south of Gwadar Bay (offshore SW Pakistan) and accompanying check-shot data and formation tops for the Gwadar-01 well (Fig. 1b). The ~40 km long dip (NE-SW) and strike (NW-SE) profiles were interpreted to define key structural and stratigraphic features in the study area. The 2D seismic data are a subset of five lines from two surveys: a 1997 survey acquired by PPL, and a survey acquired by Marathon between 1973 and 1976. Line spacing is ~2.5 km for the dip lines and ~10 km for the strike lines. The quality of the 1997 profile data was better than that from previous surveys; however, overall seismic data was difficult to interpret at depths >1s TWT due to the attenuation of amplitudes. To overcome this limitation, a time gain attribute was applied to all the lines resulting in increased interpretability. Automatic gain control (AGC) was also used to balance amplitudes across the full penetration and an example of this data conditioning is shown in Fig. 4. These attributes were applied by the authors. Seismic interpretation was also limited by the occurrence of migration smiles and fault shadow zones, particularly at depth.

Check-shot data from Gwadar-01 was utilised to tie formation tops with the seismic data (Table 1). Seismic stratigraphic units were defined based on their reflection characteristics and erosional bounding surfaces, combined with formation tops that were derived from biostratigraphic analyses of drill cuttings from Gwadar-01 (~2 km offset from line 17A: Fig. 5). The seismic units were defined as pre-kinematic if deposition of the unit pre-dated fault activity; syn-kinematic if deposition was coeval with fault activity; and post-kinematic if deposition post-dated fault activity. The timing of fault activity was deduced from the age of the associated growth strata (e.g. McClay, 1990; McClay and Ellis, 1987). Prominent structures were correlated across seismic lines, highlighting structural trends in the study region. Time structure surfaces were generated by correlating reflections across seismic lines and subsequent interpolation using standard gridding algorithms.

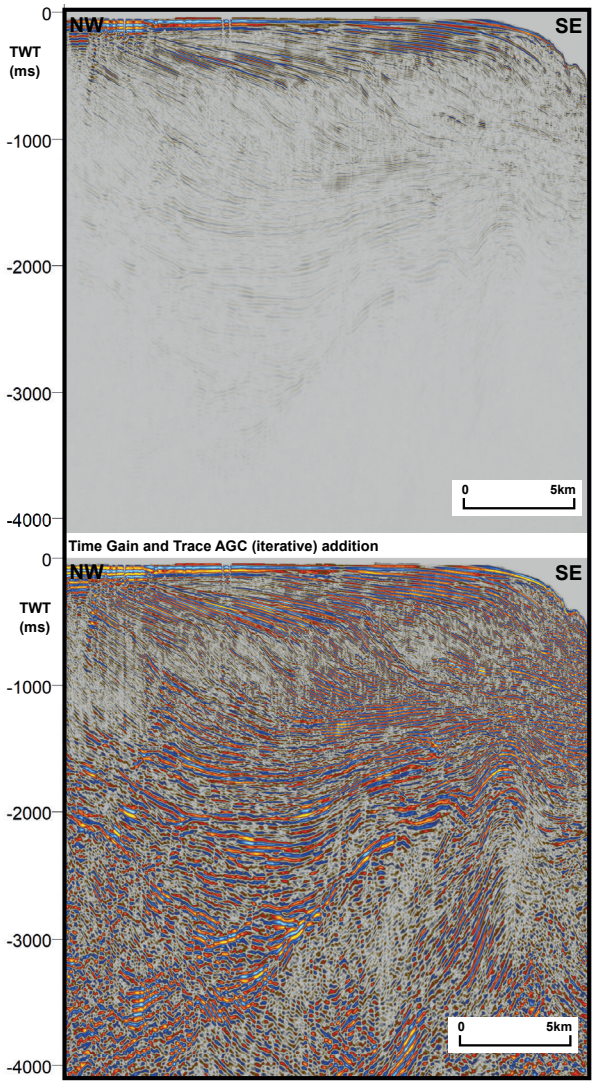

Fig. 4. Portion of a seismic section from the study area: (a) original data, and (b) conditioned data showing the effects of the time gain and trace AGC (automatic gain control) attributes.

RESULTS

Seismic stratigraphy

Seven seismic-stratigraphic units determined by reflection characteristics and erosional surfaces were identified in the study area (Fig. 5). The units are summarised below:

(i) *Pre 1 (lower Miocene – Oligocene: top is orange horizon)*: The pre-kinematic Pre 1 unit is inferred to be lower Miocene and is characterized by low-amplitude, parallel reflections which are only observed in the hanging walls of prominent thrust faults. Only the uppermost part of the unit is penetrated by well Gwadar-01, and biostratigraphic analyses suggest that the unit corresponds to the Panjgur Formation (Fig. 5).

(ii) *Pre 2 (mid-Miocene: orange – purple horizon):* This unit is inferred to be of mid-Miocene age and to correspond to the lower part of the Parkini Formation. The unit is marked by an increase in reflection amplitude and a decrease in frequencies. The absence of growth strata suggests that the unit is pre-kinematic. The unit is considerably deformed as indicated by a highly folded upper surface (Fig. 5).

(iii) *Syn 1 (upper Miocene: purple – pink horizon):* This syn-kinematic unit is characterized by continuous and high amplitude reflections that thin towards fault-propagation folds and is considered to be late Miocene in age . The base of the unit marks the syn- to pre-kinematic boundary as shown by basal reflections which onlap onto the underlying Pre 2 unit (Fig. 5). Thrust faults propagate through the unit and piggy-back basin successions (*sensu* Ori and Friend, 1984) occur in the hanging walls of these structures, providing evidence that sediment deposition was coeval with fault activity. The unit is inferred to correspond to the mid to upper Miocene Parkini Formation (Fig. 3). A prominent erosional surface marks the top of the unit, likely related to continued thrust activity and regional uplift (Fig. 5).

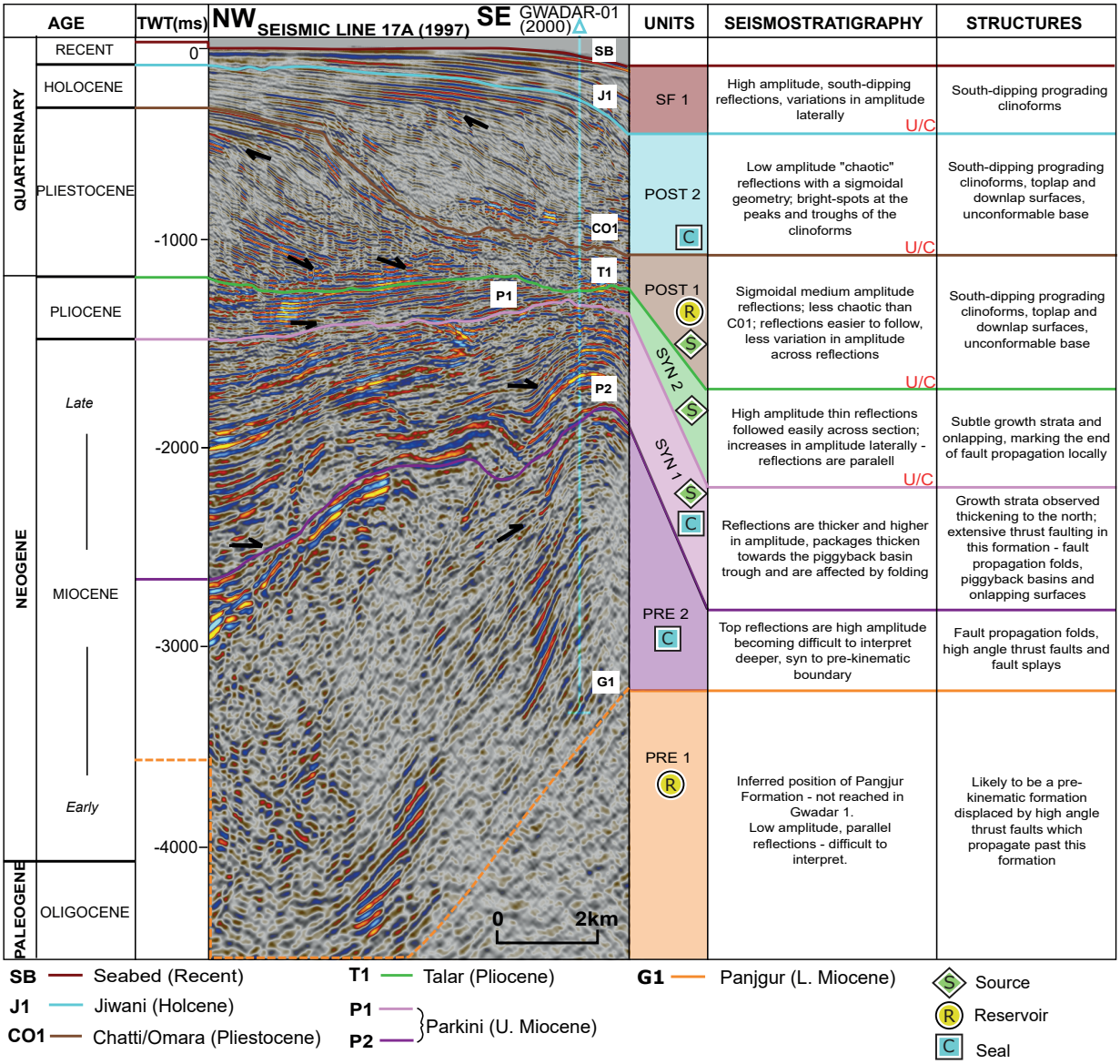

Fig. 5. Portion of seismic line 17A (profile location in Fig. 1b) showing the seismic stratigraphic units which are interpreted to occur in the study area. These comprise the pre-kinematic Pre 1 and Pre 2 units (lower Miocene – Oligocene and mid-Miocene, respectively); the syn-kinematic Syn 1 (upper Miocene) and Syn 2 (Pliocene) units; and the post-kinematic Post 1 (Pleistocene), Post 2 (Holocene) and SF 1 (Recent) units.

(iv) *Syn 2 (Pliocene: pink to green horizon)*: The syn-kinematic Syn 2 unit consists of a sequence with variable amplitude reflections and subtle growth features. The limited stratal growth compared to the Syn 1 unit may indicate decreased thrust propagation rates during deposition. High amplitude reflections occur close to fluid escape pipes and below the bottomsets of clinoforms in the overlying units. Minor growth strata and onlap surfaces at the flanks of folds are observed. The top of the unit marks the termination of fault activity in the region as the overlying units are devoid of growth strata. The unit is time-equivalent to the Pliocene Talar Formation and is widely eroded by the Post 1 unit (Fig. 5).

(v) *Post 1 (Pleistocene: green to brown horizon)*: This post-kinematic unit is characterised by sigmoidal reflections forming prograding clinoforms. Amplitudes are variable and increase in topsets and foresets in which onlap and downlap surfaces are observed, respectively. In places, the unit rests on the Syn 1 and 2 units at a major erosional surface. The absence of growth strata indicate that deposition of the unit post-dated fault activity in the study region and on this basis it is considered to be Pleistocene. The unit broadly corresponds to the Chatti and Ormara Formations.

(vi) *Post 2 (Holocene: brown – blue horizon):* This unit is characterised by low amplitude reflections forming a sigmoidal geometry which encompasses the sequence, and is bounded below by a prominent unconformity surface. Reflection amplitudes increase locally in topsets and occasionally in bottomsets. The unit is correlated with the Holocene Jiwani Formation (Fig. 3).

(vii) *SF 1 (Recent: maroon – blue horizon)*: This unit consists of shallow, high amplitude reflections forming the near-seabed stratigraphic section. The unit is affected by recent sea-floor incisions.

Margin architecture

The ~50 km long, NE-SW trending seismic line 17A images the margin from the shelf to the upper slope (Fig. 6; location in Fig. 1b). The line passes close to the Gwadar-1 well which was drilled to a depth of 3810 m (March, 2000) through an anticlinal feature interpreted as a fault propagation fold in the hanging wall of a thrust fault. Formation age at the TD was early Tortonian (late Miocene). Similar thrust faults appear to originate at depth then steepen vertically, and have a ~10 km spacing (Fig.6). In the slope area downdip from the well location, folded packages of reflections suggest multiple thrust surfaces which are interpreted as splays originating from deeper-rooted thrust faults. A similar interpretation can also be made for the structures observed in the shelf area further north, where closely-spaced splays connect with a large-scale fault at depth. The splay faults control anticlines such as the target structure for the Gwadar-1 well.

Piggy-back basin successions can be observed in the hanging walls of the thrusts, with strata thickening northwards relative to the fault planes. The growth packages have been identified by the presence of reflections onlapping onto pre-kinematic units, and by thickening of reflection packages away from faults and thinning towards fault propagation folds. Growth strata can be observed both in the hanging walls of major faults in the study area and also in the hanging walls of smaller faults.

The shelf domain is dominated at shallow depths by large-scale prograding clinoforms which rest unconformably on the syn-kinematic units characterised by prominent thrust faults, folds and piggy-back basin successions (Fig. 6). Thrusting and piggy-back basins are also common in slope areas to the south, and older units (specifically the Talar and Parkini Formations) are bounded by erosional unconformities resulting in incomplete preservation of fault propagation folds and piggy-back basin successions.

STRUCTURAL STYLES

The study area can be divided into two structural domains. In the north of the area, the upper shelf is defined by the presence at shallow depths of a thick prograding sequence with sigmoidal reflections; to the south, the "mid slope" is characterised by the absence of the prograding sequence but by the occurrence of prominent thrust faults with associated growth packages (Fig. 6). Fault propagation folds were observed in the NW-SE oriented dip lines in both the upper shelf and mid-slope domains, and affect the pre-kinematic Pre-1 to youngest syn-kinematic (Syn-2) units but not the overlying post-kinematic units (e.g. Figs 6, 7, 10). The fault propagation folds form anticlines whose axes are oriented east-west with wavelengths of ~7 km. In general, associated thrust faults dip to the north, and major thrusts have a spacing of ~10 km while smaller thrusts have a spacing of ~4 km (Fig. 10) . NW-SE seismic lines 001, 003, 008 and 17A show examples of thrust faults and associated fault propagation folds (Figs 6, 7, 8, 9,10).

Around the fault surfaces, reflections become increasingly disrupted perhaps due to fluid escape or structural complexity. Large-scale fluid escape features commonly occur at the tips of thrusts (e.g. Fig. 8: *see below*), possibly indicating fluid escape from fault propagation anticlines which may form traps in the study area. Alternatively, these features may be due to upward diapiric movement of high-pressure muds, although this explanation is less likely because growth strata are in general asymmetric (Fig. 7) suggesting a structural rather than a diapiric origin.

Piggy-back basins

Onlapping onto the topographic highs of the fault propagation folds are piggy-back basins (mini basins) which formed in the hanging walls of imbricate thrust faults (c. f. Ori and Friend, 1984; Figs 6, 7). The piggy-back basin successions demonstrate high amplitudes and continuous, onlapping reflections; onlap surfaces result from the deposition of syn-kinematic units against pre-kinematic units which were being actively thrusted. Growth strata are often horizontal at the tops of the successions, particularly in larger-scale piggy-back basins which are on average ~7 km in width and 2000 ms TWT thick (~ 2.5 km). However, smaller piggy-back basins are often tilted as a result of displacement on adjacent, larger-scale thrusts.

Strata filling the piggy-back basins comprise syn-kinematic units Syn 1 and Syn 2 of late Miocene and Pliocene ages. The occurrence of thicker growth strata in the centre of a piggy back basin suggests an important phase of structuration, with elevated fault displacements and corresponding higher rates of sediment deposition.

There is evidence to suggest that not all faults were active during the same time period. For example, profile 001 (Fig. 7) shows the occurrence of piggy-back basin successions in the hanging walls of thrust faults across the entire section; syn-kinematic packages have also been correlated across the section. In the NW of the figure, the Syn 1 unit (Fig. 5) demonstrates growth features which suggest that the bounding fault was undergoing significant propagation around the time of deposition in the late Miocene. However, the Syn-2 unit overlying the fault does not display significant

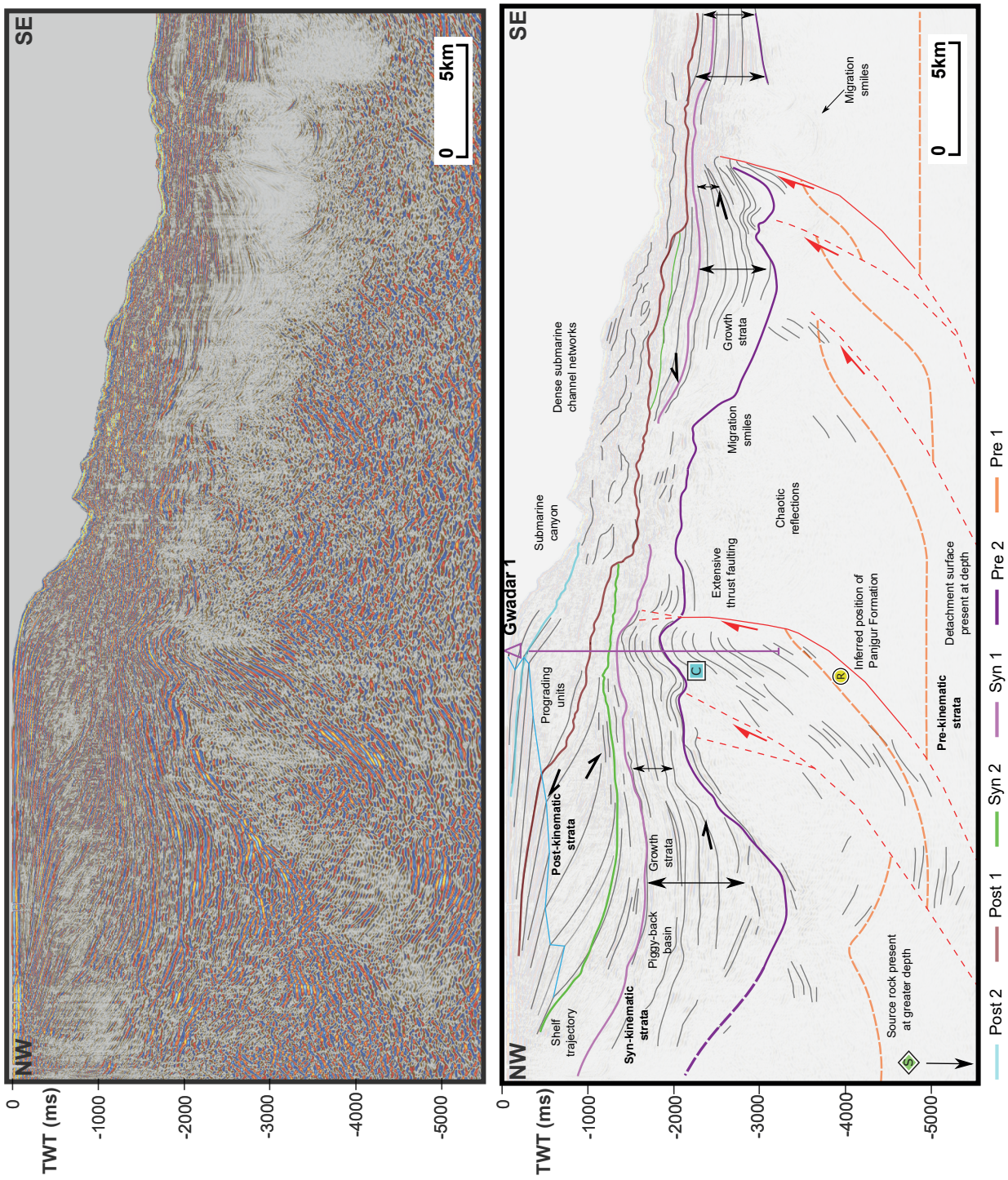

Fig. 6. Uninterpreted and interpreted regional dip line 17A (1997 survey) (profile location in Fig. 1b). Unit boundaries, key structures and petroleum systems elements are labelled.

growth, suggesting that fault propagation ceased before the Pliocene. A major fault in the SE of the profile also displays an associated piggy-back basin succession, but here the Syn-2 unit shows thinning of reflections towards the fault plane and the occurrence of growth strata. This suggests that propagation of the fault continued from the late Miocene to the Pliocene. Thus the two faults were both active in the late Miocene, but only the SE fault continued to propagate throughout the Pliocene while the NW fault remained inactive.

Post-kinematic prograding units and erosional surfaces

A post-kinematic Pleistocene to Recent prograding interval is observed at shallow depth in the shelf region in the north of the study area (Fig. 6) and comprises the Post 1, Post 2 and SF 1 seismic stratigraphic units (Fig. 5). Clinoforms in this interval extend down to 2s TWT (~2.5 km depth) and can be traced north-south for ~30 km (Figs 6, 7, 8, 9), illustrating shelf progradation over time. Older prograding units exhibit brightening

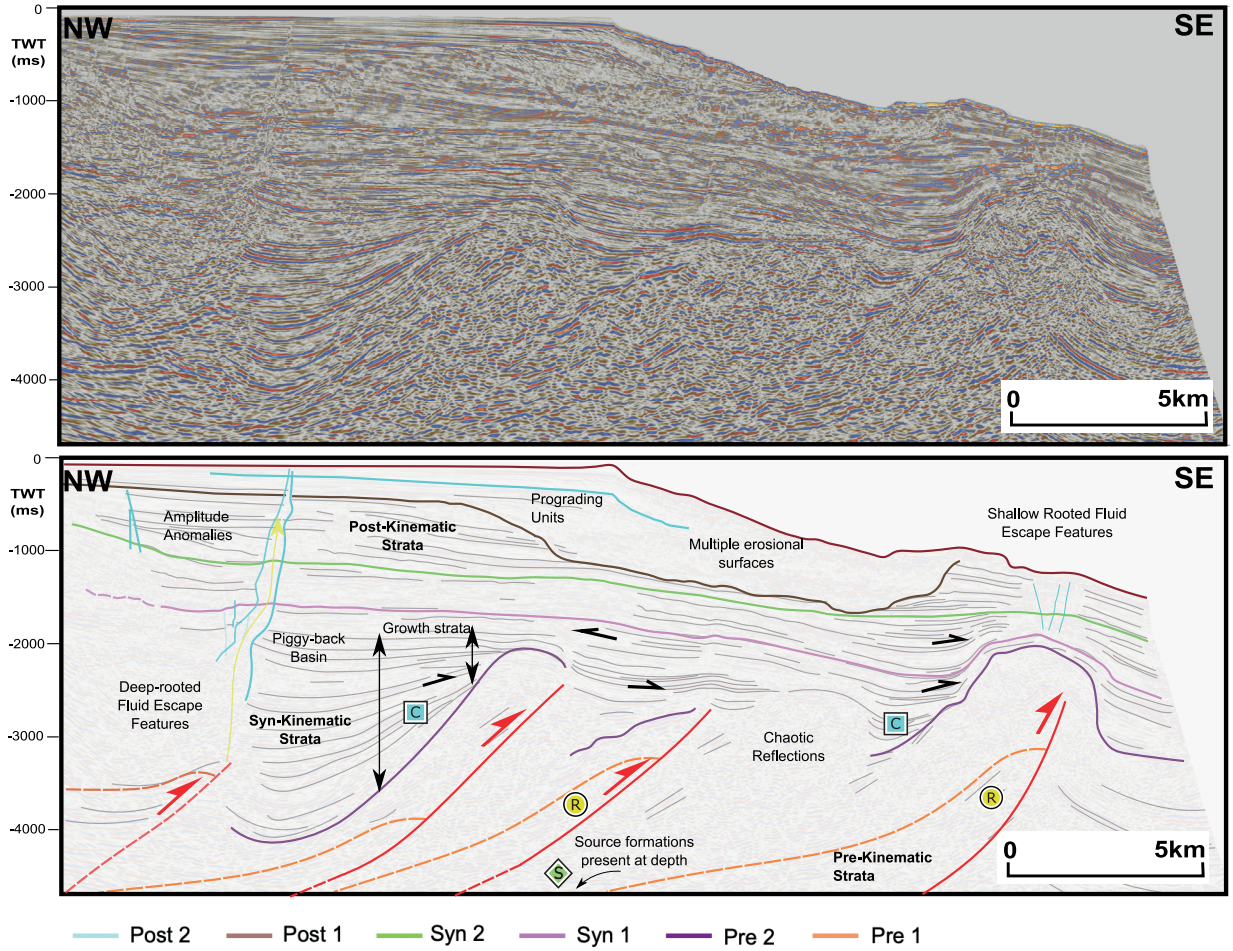

Fig. 7. Uninterpreted and interpreted regional dip line 001 (1997 survey) (profile location in Fig. 1b). Unit boundaries, key structures and petroleum system elements are labelled.

of reflections in clinoform bottomsets and foresets with more chaotic reflections observed in slope segments (Figs 7, 8). Brightening occurs adjacent to fluid escape features which commonly propagate through the prograding interval (e.g. "Amplitude anomalies" on Fig. 8). The southerly direction of progradation indicates sediment input from the north.

Marked erosional surfaces have been mapped within the prograding interval and in places cut deeply into the underlying syn-kinematic succession, forming submarine canyons which can be seen on strike lines (Fig. 11). The canyons are 1-3 km across and are in general oriented north-south (Fig. 11). They are interpreted to be filled with sediments of the Post 1 seismic stratigraphic unit corresponding to the Holocene Jiwani Formation (Fig. 5).

Fluid escape pipes

Near-vertical or columnar zones of reflection disruption are commonly observed in the study area (Figs 7 and 8) and define the locations of fluid escape pipes (*sensu* Cartwright *et al.*, 2007) which are interpreted to result from the upward migration of overpressured fluids and subsequent fracturing of host sediments (Fig. 12a). Fracturing and disruption of stratigraphy is demonstrated by the variance attribute display (Fig. 12b). Fluid escape pipes were divided into large-scale features, which appear to originate at depth, and smaller-scale features which are constrained to the upper parts of the seismic profiles corresponding to the Pliocene to Recent stratigraphy.

Large, deep-rooted fluid escape pipes are ~2.5 km across at the base, thinning upward to widths of less than 0.5 km (Figs 8, 12). In general, they do not appear to reach the sea floor and exhibit velocity sag or pull down, perhaps indicating fluid migration. In Fig. 12, a vertical pipe appears to propagate through the tip of an interpreted thrust fault; similar pipes originating from deep structures can be observed on all the NW-SE seismic lines (Figs 6-9). The structure in Fig. 12 is interpreted as a breached fault propagation fold from which fluids have migrated vertically upwards to the surface through a number of pipes. The fluid escape features therefore illustrate a lack of seal integrity in the anticlinal fold. As a fluid escape pipe is followed up-section, adjacent reflections appear locally to show increases in amplitude (Figs 7 and 12).

Comparable but smaller-scale fluid escape pipes, also associated with fault propagation anticlines, are observed further down dip, away from the shelf break,

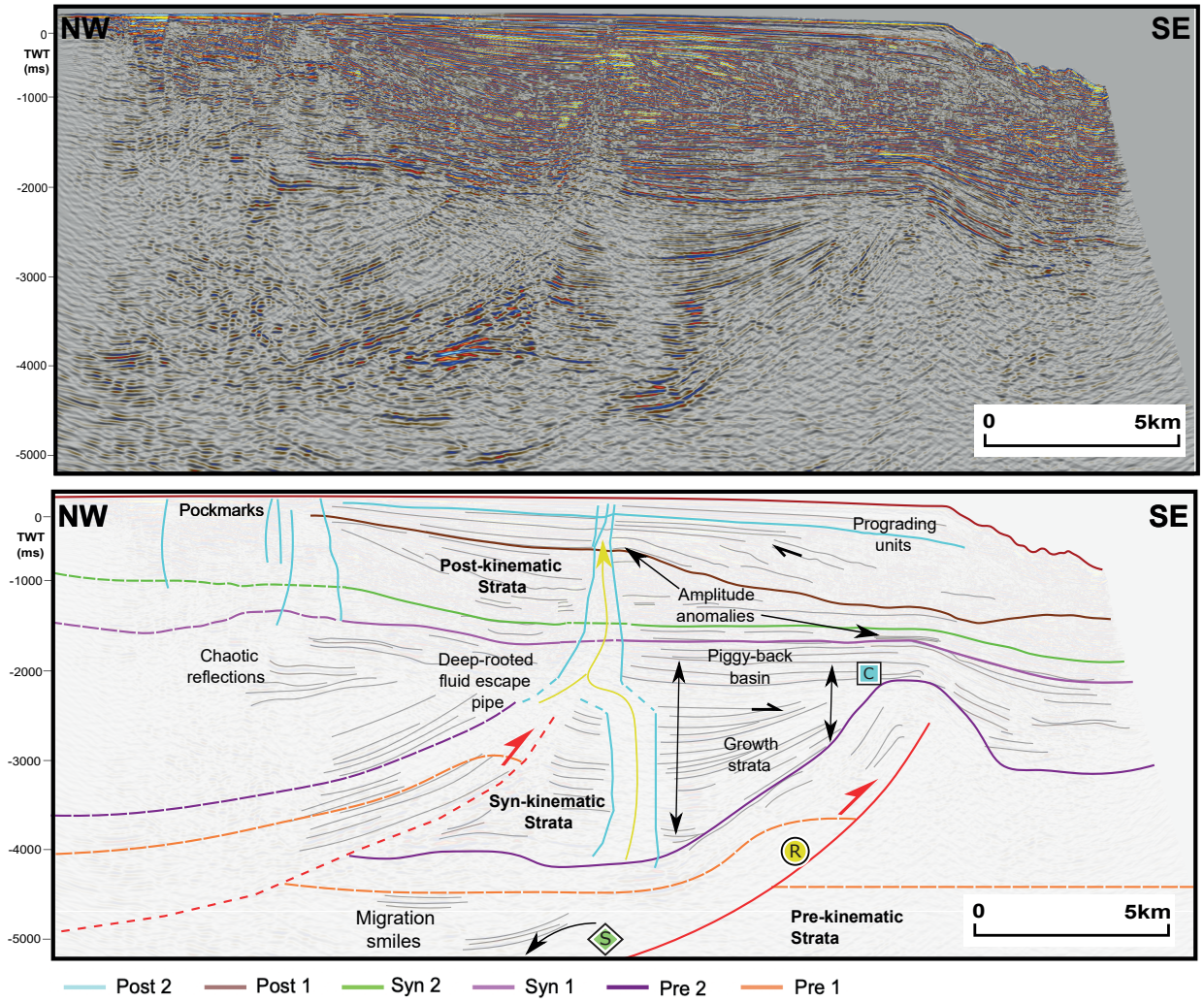

Fig. 8. Uninterpreted and interpreted regional dip line 003 (1997 survey) (profile location in Fig. 1b). Unit boundaries, key structures and petroleum system elements are labelled.

and are also found in the prograding units (Fig 7). The smaller-scale pipes are in the order of 100 m in width and occur within the prograding Pleistocene to Recent succession in the shelf region to the north of the study area (Figs 8 and 9). Also within the prograding interval are a series of linear horizontal features, identified by distortions and velocity sags in the reflections similar to the larger escape features, but with a shorter length and thickness. These features appear locally to have reached the seafloor where they form shallow depressions and pockmarks (Figs 7, 8, 9).

Amplitude anomalies

Prominent amplitude anomalies are commonly observed on seismic profiles in the study area. For example, dip line 003 (Fig. 8) shows the presence within the Pliocene Syn 2 Unit of an abnormally high-amplitude horizontal reflection directly above a fault propagation fold (Fig. 13). The amplitude anomalies are often located at the apices of, or adjacent to, fluid escape pipes (e.g. Fig. 12). Onlaps within the Pliocene Syn 2 unit are observed updip of the amplitude anomalies (Fig. 13), and subtle velocity sags occur below them. As elaborated in the Discussion below, these high amplitude events could indicate the presence of hydrocarbons, with the potential for combined structural-stratigraphic traps in pinch-outs onto the folds.

DISCUSSION

Evolution of the Makran

Fig. 14 summarises the evolution of the Makran accretionary wedge offshore Pakistan since the Late Cretaceous based on previous publications and consistent with the results of this study. Intra-oceanic subduction took place between the Late Cretaceous and the Eocene (Fig. 14a) but without the development of an accretionary wedge (Burg, 2018). North of the subduction zone, the Bajan Durkan volcanic arc developed and is preserved in onshore Pakistan; back-arc extension occurred further north. No sediments of Eocene or older ages have yet been interpreted to be present in the Makran from seismic or well data.

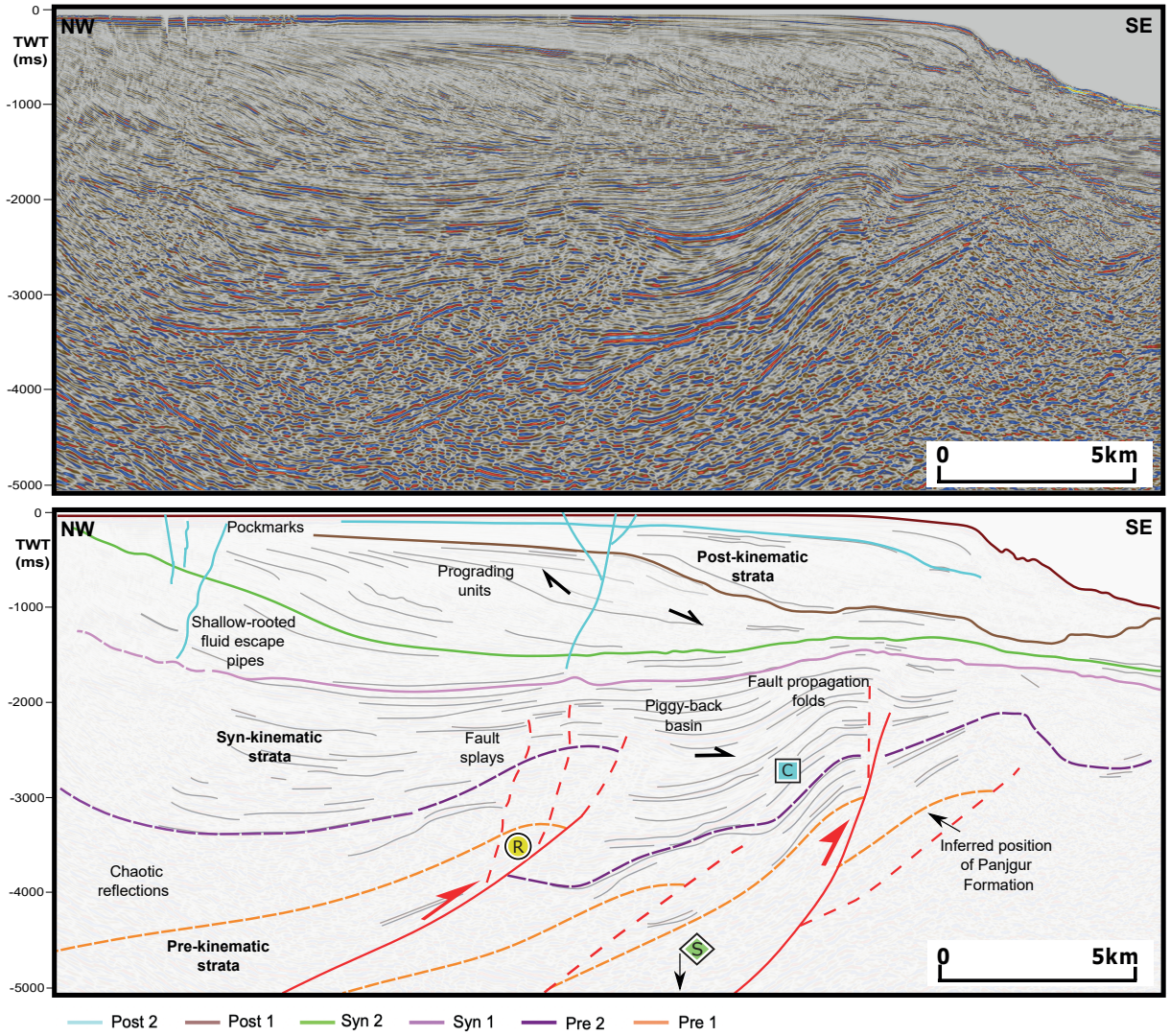

Fig. 9. Uninterpreted and interpreted regional dip line 008 (1997 survey) (profile location in Fig. 1b). Unit boundaries, key structures and petroleum systems elements are labelled.

Eocene – mid-Miocene (Fig. 14a): Accretionary wedge formation began in the Eocene (Byrne *et al.*, 1992, Schlüter *et al.*, 2002) (Fig. 14a), at the same time as uplift and erosion of the Himalayas provided detrital sediments to the palaeo- Indus River system to the east of the Makran (Grigsby *et al.*, 2009). These detrital sediments were then re-deposited in the Makran area forming the distal shales of the Hoshab Formation and the basin-floor turbidites of the Panjgur Formation. Imbricate faulting occurred to the north of the Makran but the accretionary wedge was not yet developed and the deformation front had not reached as far south as the study area. This is evidenced by the absence of growth strata in the mid-Miocene and older intervals in the study area (Figs 5, 6).

Mid-Miocene – Pliocene (Fig. 14b): In the mid-Miocene, widespread thrust faulting occurred in the study area due to renewed subduction of the Arabian Plate beneath the Eurasian margin causing an increased rate of accretion (Burg, 2018). Observations in this study suggest that the onset of thrust faulting occurred during the deposition of the mid-upper Miocene Parkini Formation which corresponds to the syn-kinematic Syn 1 unit (Fig. 5). The unit displays growth stratal geometries and onlapping terminations onto pre-kinematic fault propagation folds (Figs 6-9), indicating that thrust faults were active during deposition. This observation is broadly consistent with the growth packages recorded by Grando and McClay (2007) in the western Makran, which suggests a younger syn-kinematic sedimentary succession and frontal accretion from the early to late Miocene.

In the study area, all the thrust faults are interpreted to originate from a detachment surface which is likely located in the pre-kinematic Hoshab Formation shales (Platt *et al.*, 1985). It is proposed that this faulting was synchronous with complex faulting of the deeper sedimentary interval and marks the initiation of sediment underplating within the Makran region.

Syn-kinematic deposition continued through the Pliocene as suggested by the presence of growth packages within the equivalent Talar Sandstone.

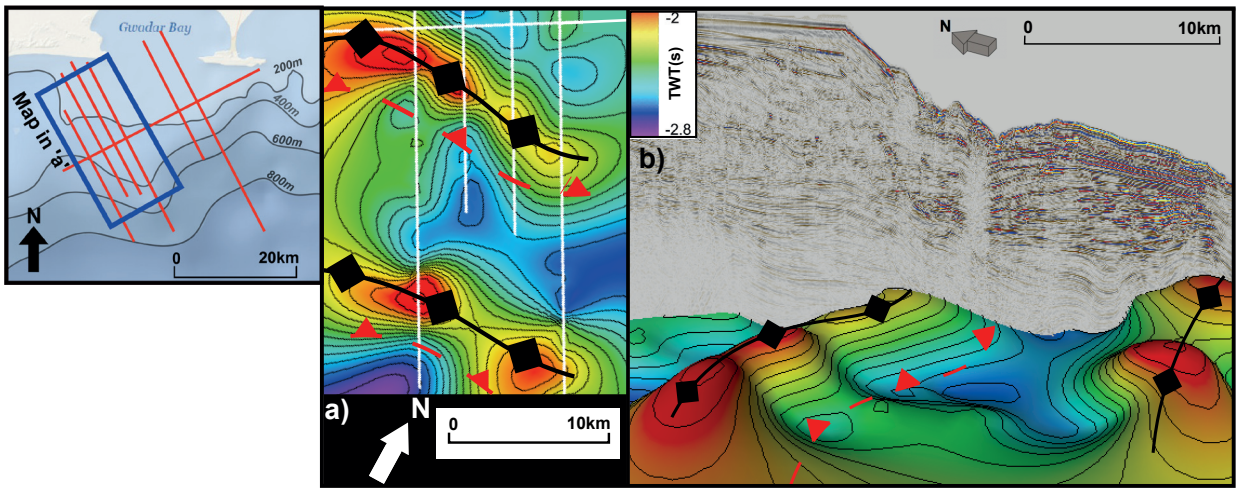

Fig. 10. (a) Time structure map of the top- Pre 2 unit (Parkini Formation, upper Miocene) showing the presence of fault propagation folds in the study area. The location is shown in the inset map to the left. (b) 3D view of the top- Pre 2 unit showing the presence of fault propagation folds affecting the Miocene interval, as evidenced in seismic line 007.

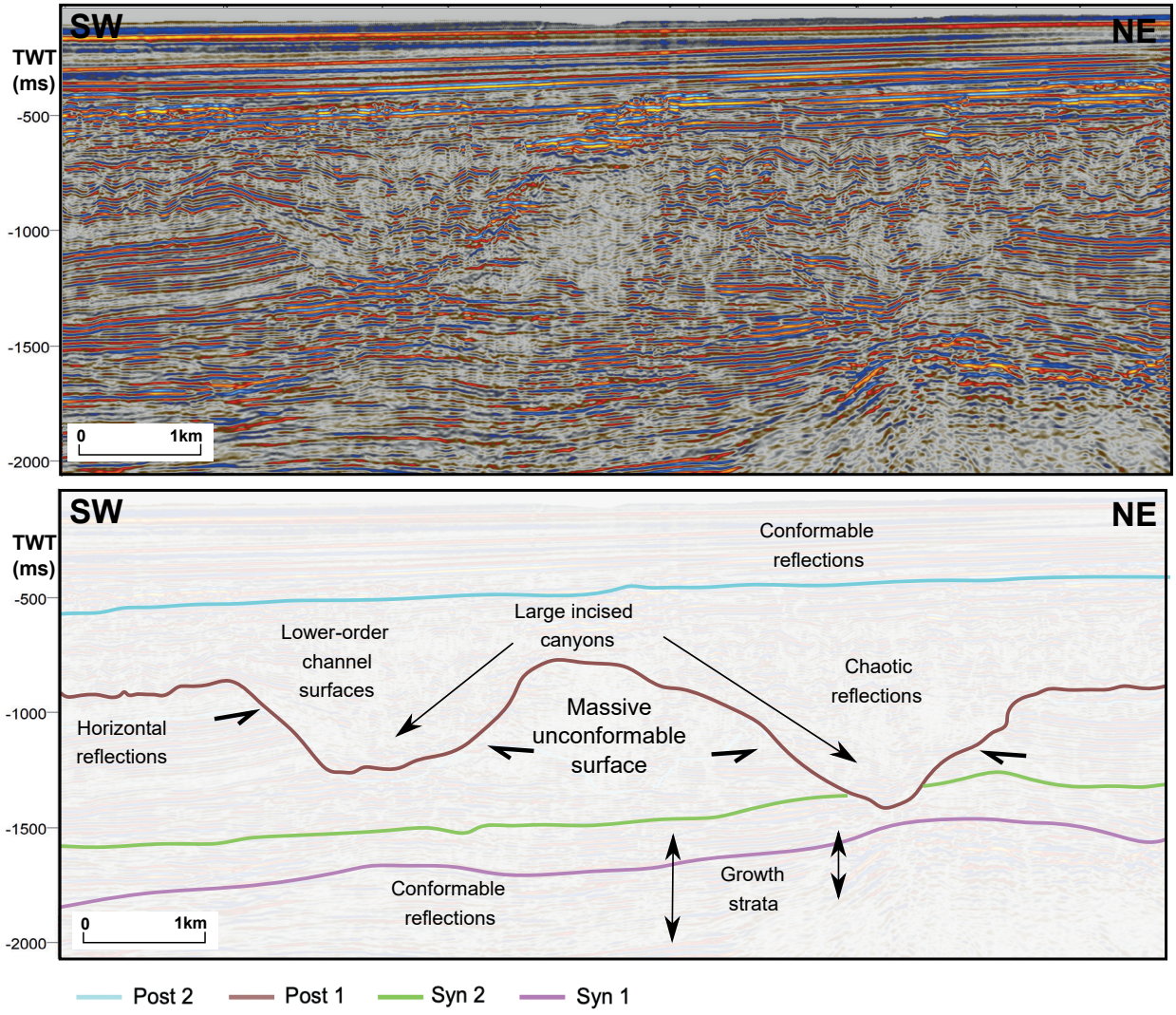

Fig. 11. Uninterpreted and interpreted excerpt from seismic line 006 (1997 survey) showing submarine canyons marking the top of the Post 1 unit (top Pleistocene).

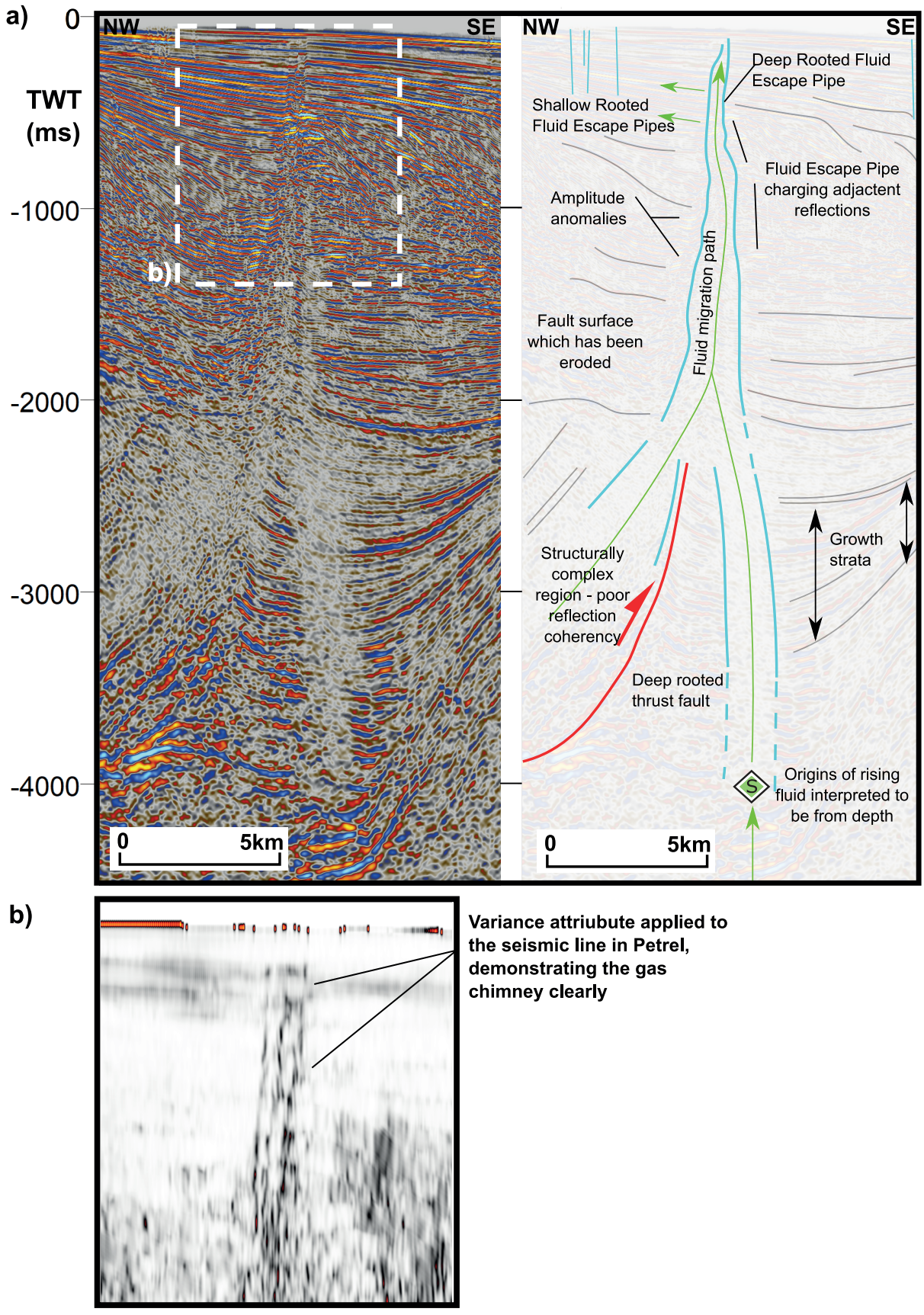

Fig. 12. (a) Uninterpreted and interpreted excerpt from seismic line 003 (1997 survey) showing a deep-rooted fluid escape pipe.
(b) Application of the variance attribute provides a clearer interpretation of the fluid escape pipe, together with fracturing and disruption of the stratigraphy.

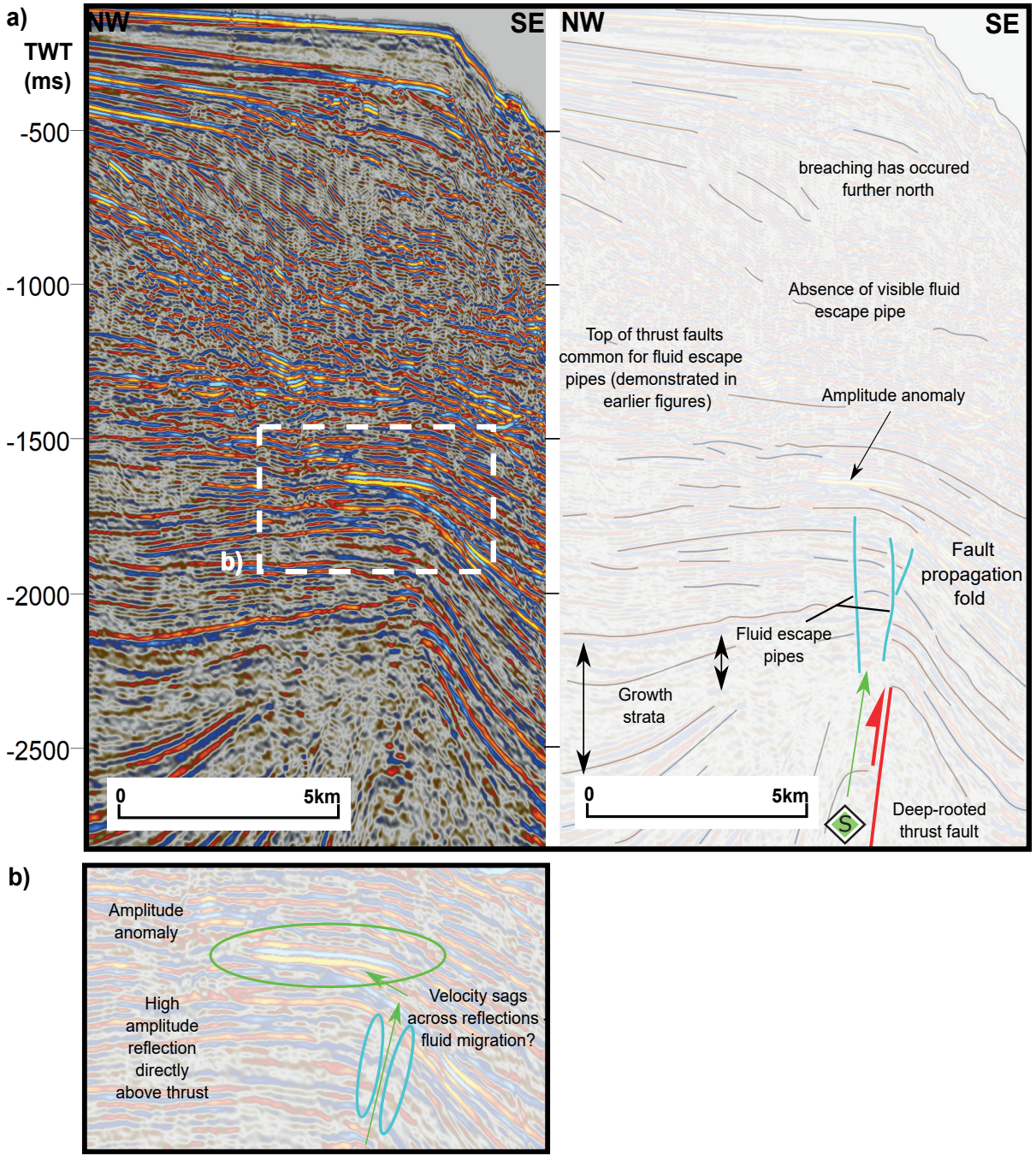

Fig. 13. (a) Uninterpreted and interpreted section from seismic line 003 (1997 survey) illustrating a bright spot above a fault propagation fold whose crest is cut by a fluid escape pipe; (b) zoomed-in view of the amplitude anomaly.

Pliocene growth is mainly observed to be associated with deformation on seaward faults (i.e. those located to the south) within the Syn-2 unit (e.g. Fig. 7). This is interpreted to have been caused by secondary fault activation after periods of quiescence as the Makran deformation front migrated to the south of the study area. Southward migration of the Makran front was also noted by Smith *et al.* (2012).

Pleistocene – Recent (Fig. 14c): By the end Pliocene, observations in this study show that faulting in the study area had ceased, and the active deformation front had therefore likely migrated further south. The cessation of faulting is evidenced by the presence of an undeformed prograding interval which seals folds and piggy-back basin successions (Figs 6-9). The end of compression in the proximal part of the margin in the late Pliocene is also indicated by the activation at this time of listric extensional faults in shelfal parts of the Iranian Makran (Grando and McClay, 2007). The extension could have resulted from gravitational collapse as the deformation front migrated southwards (e.g. Platt 1986; Rowan *et al.*, 2011). However, such extensional structures are not observed in the study area.

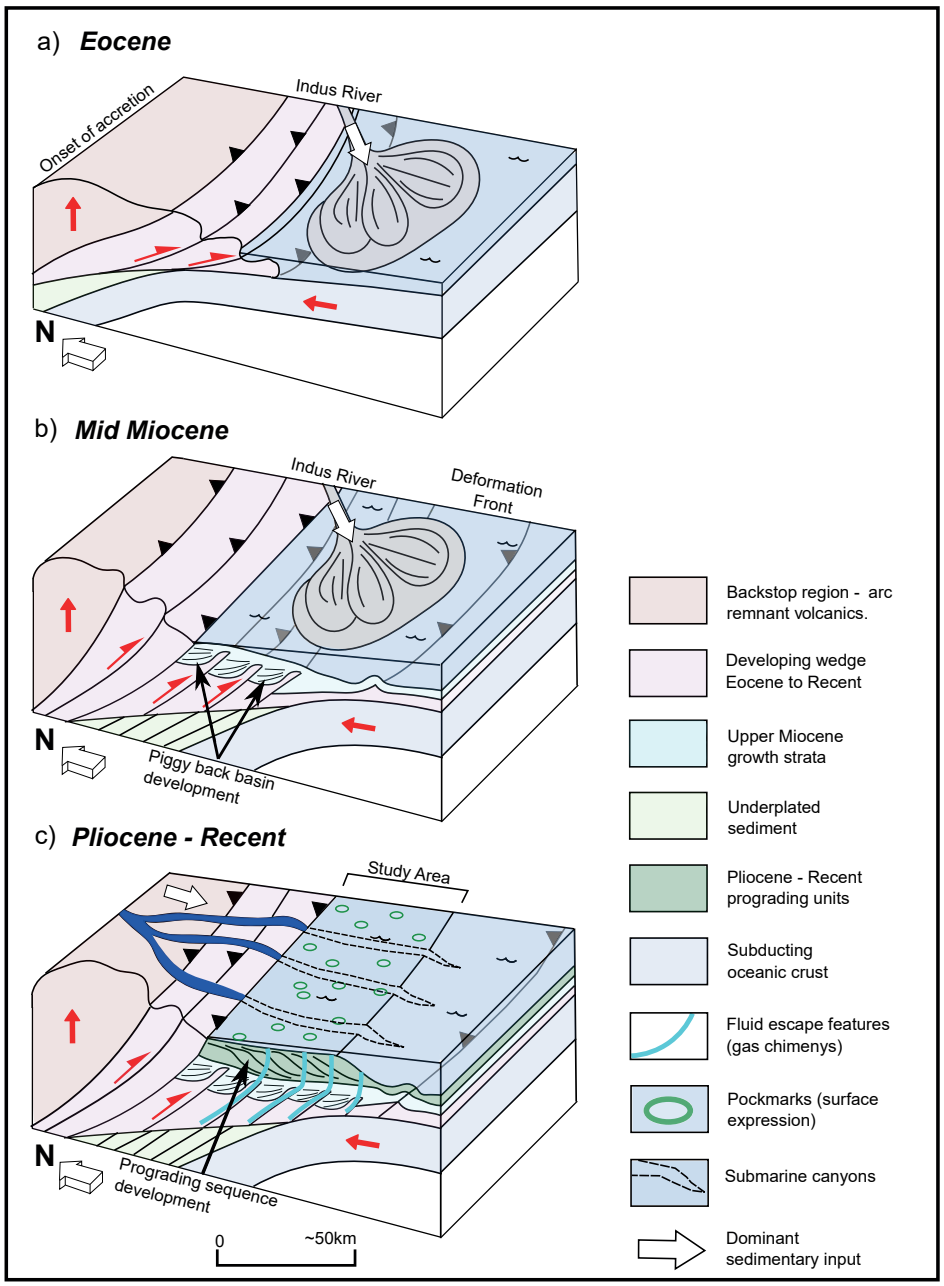

Fig. 14. Block diagrams illustrating the tectonostratigraphic evolution of the study area in the Makran accretionary prism in the (i) Eocene; (ii) mid-Miocene and (iii) Pliocene – Recent. See text for details.

The Pliocene to Recent prograding interval, ~2 TWT ms (~2.5 km) thick, marks a change in the dominant sedimentary input. The prograding units have not been identified in previous investigations but are clearly identifiable on the seismic profiles studied. Deposition of the prograding units was a result of regional uplift and erosion associated with increased accretion of the Makran, which consequently resulted in a major influx of detrital sediment via rivers into the study area.

Fluid escape features

Extensive fluid escape features were observed in the seismic profiles studied, and indicate periods of fluid migration probably related to the occurrence of widespread overpressuring in the Makran accretionary prism. Overpressures here are a major hindrance to exploration and have caused a number of wells to fail to reach their target depths (Hussain *et al.*, 2015; Bernud *et al.*, 2000). The occurrence of deep-rooted fluid escape pipes at depth (Fig. 12) suggests a major phase of fluid migration.

Fluid escape features have not previously been reported in the upper shelf of the Makran, although gas features have been identified towards the deformation front (Grando and McClay, 2007; Liu *et al.*, 2020). In the study area, both deep-rooted and shallow-rooted fluid escape pipes are observed. The deep-

rooted features appear to terminate in the Holocene section and are not associated with sea-floor relief or pockmarks. By contrast the shallow-rooted features, which are an order of magnitude smaller than the deep-rooted features, often reach the sea floor. Some of the shallow-rooted fluid escape pipes are located in close proximity to larger, deep-rooted features (e.g. Figs 7, 8, 12), perhaps indicating the transfer of pressure into higher stratigraphic intervals (Elger *et al.*, 2018).

The fluid escape features together with amplitude anomalies observed on seismic profiles suggest that the migration and accumulation of hydrocarbons has occurred in this part of the Makran. Gas shows have been reported in exploration wells in the area. For example, in well Gwadar-1, biogenic methane was reported at depths of up to ~2500 m as suggested by carbon isotope analyses. However, headspace gas analyses from depths greater than 2680 m pointed to an increase in the presence of C_2 through C_5 hydrocarbons, indicating a thermogenic origin. Furthermore, analysis of mud volcanoes (such as the Omara mud volcano: Wiedicke *et al.*, 2001) and gas seeps have demonstrated the presence of both biogenic (Delisle *et al.*, 2004) and thermogenic hydrocarbons (Harms *et al.*, 1984, Khan *et al.*, 1991).

Relating these observations to the fluid escape pipes, it is proposed that the deep-rooted features are likely to result from the upward movement of thermogenic hydrocarbons sourced from depth, whilst the more shallow features are probably associated with biogenic gas. Thermally mature source rocks are believed to be present at depth in the high-TOC shales of the Oligocene Hoshab Formation (Harms *et al.*, 1884, Hussain *et al.*, 2015), which are overlain by thick turbidite sandstones in the Miocene Panjgur Formation forming the main reservoir target (Fig. 3).

Submarine canyons

The large-scale unconformable surfaces observed in the Post 2 unit (Figs 8-11) highlight the onset of an important developmental phase in the region. The presence of submarine canyons indicates a significant increase in sediment delivery, possibly coinciding with a period of uplift and denudation in the Makran ranges and also with a phase of eustatic sea-level fall from Pliocene to Recent time (Miller *et al.*, 2005). Within the canyons, seismic packages of a chaotic nature are often observed and may be interpreted as slumps and debris flows.

Canyons resulting from slope failure are often found in active fold-and-thrust belts and may be triggered by seismicity (e.g. Strozyk *et al.*, 2010). Slope collapse and resulting canyon formation is accentuated by uplift as well as by weakening of the sedimentary units by fluid seeps (Elger *et al.*, 2018), as has been observed in the Cascadia Accretionary Complex (McAdoo *et al.*, 2003). A similar mechanism for canyon formation may have occurred in the Makran region, where there has been frequent seismic activity over the past 100 years including earthquakes with magnitudes exceeding Mw 8 (Mokhtari *et al.*, 2019). A particularly high frequency of earthquakes has been recorded in and around the study area (Nemati, 2019). Canyon formation in this region may therefore have resulted both from eustatic sea level fall in the Holocene and slope failure related to sediment weakening and seismicity.

Hydrocarbon prospectivity

Exploration in the Makran has been challenging to-date but accretionary wedges elsewhere may provide analogues in terms of prospectivity. Thus limited volumes of oil and gas have been found in accretionary prims in Seram Island (Indonesia) and in the Cascadia subduction zone, NW USA (Hessler and Sharman, 2018), while more major hydrocarbon discoveries have been made in convergent settings such as the Cook Inlet Basin in Alaska which has reserves estimated to total about 1.3 MM brl o.e. and where 8.5 TCF gas had been produced as of 2017 (Redlinger *et al.*, 2018).

The main challenges for hydrocarbon exploration in accretionary wedges relate to structural complexity and to the depth and quality of the reservoir facies (Hessler and Sharman, 2018). In the Makran, the high reservoir qualities associated with onshore outcrops of the lower Miocene Panjgur Formation sandstones have not been identified in offshore wells. Structural complexity may also have hindered identification of reservoir facies. However, amplitude anomalies associated with fluid escape pipes are widely observed on seismic sections (e.g. Fig. 13) and are interpreted to indicate vertical hydrocarbon migration from a thermally mature source rock, inferred to be the Oligocene Hoshab Shale Formation. The distribution and maturity of source rocks in the offshore Makran are poorly understood and require further detailed investigation.

In addition, brightening observed in Pleistocene clinoforms adjacent to shallow fluid escape pipes may represent charging by migrating hydrocarbons originating from shaly source rocks in distal slope facies. After expulsion, these hydrocarbons would have migrated up-dip. Alternatively, the shallow fluid escape features may have developed from the deeper, larger-scale fluid escape pipes which charged top-set strata with hydrocarbons which then migrated laterally, forming minor pipes. This is evidenced by the presence of bright reflections which are often observed adjacent to the pipes, but which are not observed down-dip in the prograding units.

Fig. 15 illustrates a cartoon play cross section for the study area. Potential structural traps consist of 4-way anticlines formed as a result of thrust fault propagation. Risks related to exploration of these

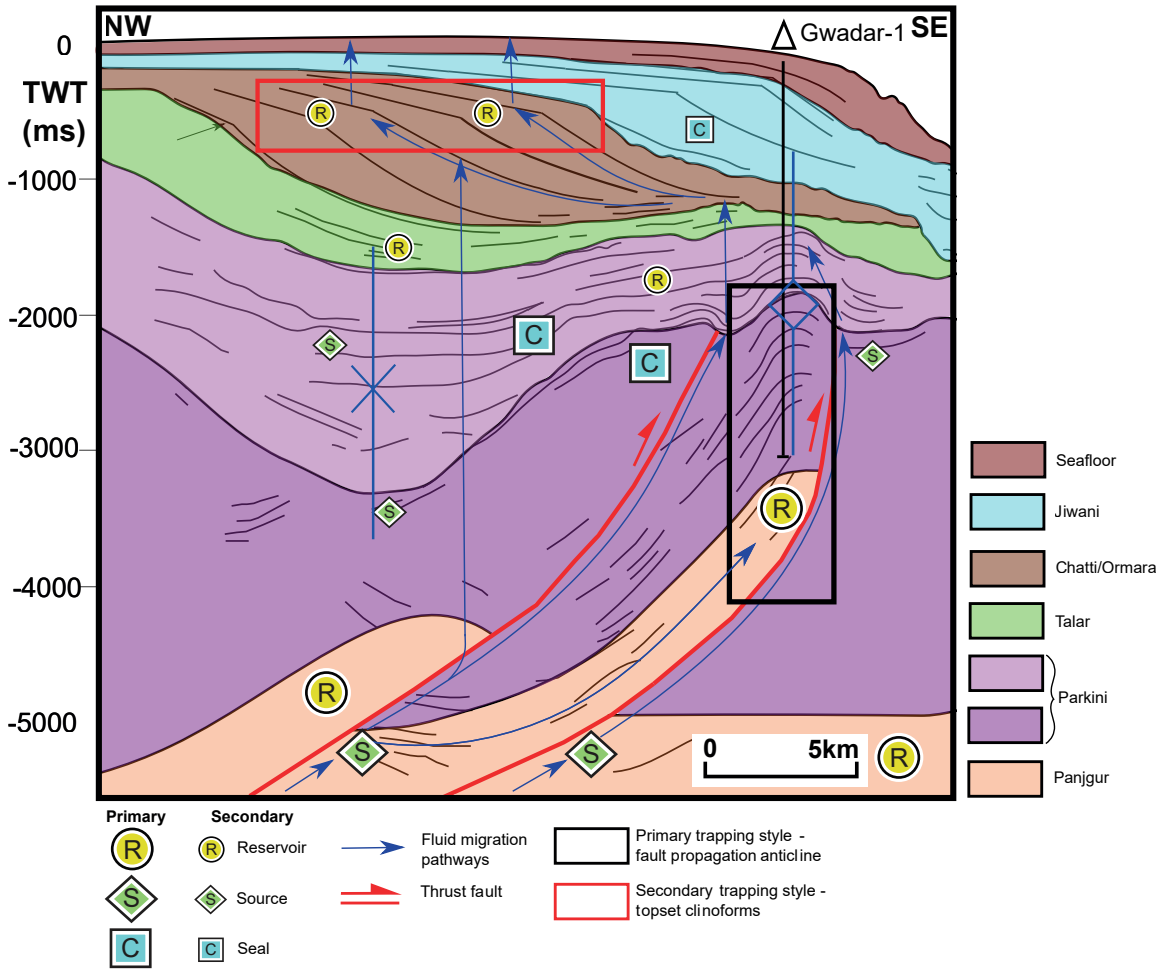

Fig. 15. Play summary cartoon for the study area showing the principal petroleum systems elements (source, reservoir and seal) and possible migration pathways. The cartoon shows the structural play (black rectangle) targeted by the Gwadar-1 well which is interpreted as a fault propagation anticline containing thermogenic hydrocarbons sourced by Oligocene shales in the Hoshab Formation. A biogenic play may also be present (red rectangle). See text for details.

structures include absence of the Panjgur Formation reservoir, although it may be present at great depth. The presence of a mature source rock (Hoshab Shales) is indicated by shows of thermogenic gas in wells drilled in the area; upward migration of thermogenic hydrocarbons may have resulted in the formation of the observed deep-rooted fluid escape pipes. A seal is provided by the thick mudstones in the Parkini Formation, which rests directly above the Panjgur Formation (Kahn *et al.*,1991) and which may also have minor reservoir and source rock potential (estimated depth at 5000 ms (TWT) is ~6000 m).

Potential stratigraphic trapping may occur within the Pleistocene post-kinematic succession (Chatti and Omara Formations) as suggested by brightening of clinoforms up-dip from, and adjacent to, shallow fluid escape pipes. The presence of hydrocarbons in this succession is indicated by both amplitude anomalies and fluid escape features such as seafloor pockmarks. The hydrocarbons are biogenic and sourced from distal, organic-rich mudstones in bottomset strata. Reservoir rocks could consist of upper shoreface sandstones with variable reservoir potential. An analogue play may be present in the Meren field in the offshore Niger Delta (Esan, 2004) where an estimated 1.3 billion barrels of oil are in place (Poston *et al.*, 1983) and which produces from stratigraphic traps similar to those observed in the study area.

A conceptual trap is present in the submarine canyons observed in strike lines (Fig. 11). A secondary reservoir target consists of the well-sorted sandstones of the Talar Formation which lie above the Parkini Formation. These sandstones could be sealed by overlying lower slope mudstones and charged by source rocks in the Hoshab and Parkini Formations.

CONCLUSIONS

The structures and seismic stratigraphy of the Makran accretionary wedge offshore Gwadar Bay (SW

Pakistan) were investigated using 2D seismic profiles calibrated with subsurface data from the Gwadar-01 well. The main results of this study can be summarised as follows:

• A series of thrust and associated fault propagation anticlines with fold axes ~7 km long and wavelengths of ~10 km are observed in the Oligocene – upper Miocene succession, and define the structure of the accretionary wedge in the study area.

• A phase of accelerated accretion in the late Miocene is indicated by the occurrence of piggy-back basins containing well-developed growth strata of the same age.

• From the Pleistocene, faulting had ceased in the study area as the deformation front of the accretionary wedge moved southward.

• The occurrence of Pliocene canyons and prograding units indicates sediment input from the north. Canyons are inferred to have developed during a phase of low eustatic sea-level as a result of slope collapse due to weakening of shelfal sediments due to rising fluids in escape pipes as well as to regional uplift and seismicity.

• The presence of Holocene to Recent fluid escape pipes supports the interpretation of fluids originating from significant depths. Shallower features such as pockmarks have also been observed.

• The fluid escape pipes could suggest the possible presence of hydrocarbon accumulations in the accretionary prism, and amplitude anomalies and bright spots were observed adjacent to these features.

• Fault propagation anticlines remain primary targets for exploration, but further investigation could also focus on structures that lack evidence of a seal breach (i.e. fluid escape pipes originating from fold crests). Thus possible reservoir targets have been identified in the Talar Formation and in topsets in the Chatti and Omara Formations.

ACKNOWLEDGEMENTS

The authors would like to recognise Pakistan Petroleum Limited (PPL) and the Directorate General of Petroleum Concession (DGPC) – Ministry of Energy, Pakistan – who are thanked for providing the data and supporting the research. Resources and equipment were kindly provided by the Department of Earth Science at Royal Holloway, University of London where the research was developed as part of an independent student project for the MSc. programme in Petroleum Geoscience. Schlumberger and Dr Leigh Truelove are thanked for providing the subsurface interpretation package Petrel. Thorough reviews by Stuart Burley, Alan MacGregor and an anonymous referee improved the paper and are acknowledged with thanks.

Data reference

All 2D seismic and well data was provided by Pakistan Petroleum Limited (PPL: 4th Floor, PIDC House, Karachi 75530, Pakistan) and the Directorate General of Petroleum Concession (DGPC: Ministry of Energy, Pakistan).

REFERENCES

AHMED, S.S., 1968. Tertiary Geology of Part of South Makran Baluchistan, West Pakistan. *AAPG Bull.,* **53**, https://doi.org/10.1306/5D25C863-16C1-11D7-8645000102C1865D

BACK, S. and MORLEY, C. K., 2016. Growth faults above shale – Seismic-scale outcrop analogues from the Makran foreland, SW Pakistan. *Mar. Petrol. Geol.,* **70**, 144-162. https://doi.org/10.1016/j.marpetgeo.2015.11.008

BENRUD, M.S., KITSON, A., EMERY, J., CAVANAGH and BYRD, D., 2000. Gwadar-1 Final Geological Report. *Unpublished.*

BURG, J.-P., 2018. Geology of the onshore Makran accretionary wedge: Synthesis and tectonic interpretation. *Earth-Sci. Rev.*, **185**, 1210-1231. https://doi.org/10.1016/j.earscirev.2018.09.011

BYRNE, D.E., SYKES, L.R. and DAVIS, D.M., 1992. Great thrust earthquakes and aseismic slip along the plate boundary of the Makran Subduction Zone. *Journ. Geophys. Res.*, **97 (B1)**, 449-478. https://doi.org/10.1029/91JB02165

CARTWRIGHT, J., 2007. The impact of 3D seismic data on the understanding of compaction, fluid flow and diagenesis in sedimentary basins. *Journal of the Geological Society,* **165**(5), 881-893, https://doi.org/10.1144/0016-,6492006-143

CHEEMA, M. R., RAZA, S. M. and AHMAD, H., 1977. Stratigraphy of Pakistan. *Geological Survey of Pakistan, Memoirs,* **12**, 56-98. Quetta.

CRITELLI, S., DE ROSA, R. and PLATT, J.P., 1990. Sandstone detrital modes in the Makran accretionary wedge, southwest Pakistan: implications for tectonic setting and long-distance turbidite transportation. *Sediment. Geol.,* **68**, 241-260. https://doi.org/10.1016/0037- 0738(90)90013-J

DELISLE, G., 2004. The mud volcanoes of Pakistan. *Environ. Geol.* **46**, 1024-1029. https://doi.org/10.1007/s00254-004-1089-x

DELISLE, G., VON RAD, U., ANDRULEIT, H., VON DANIELS, C.H., TABREZ, A.R. and INAM, A., 2002 Active mud volcanoes on- and offshore eastern Makran, Pakistan. *Int. Journ. Earth Sciences*, **91**, 93-110 https://doi.org/ 10.1007/s005310100203

DEMETS, C., GORDON, R.G., ARGUS, D.F. and STEIN, S., 1990. Current plate motions. *Geophys. Journ. Int.* **101**, 425-478. https://doi.org/10.1111/j.1365-246X.1990.tb06579.x

DEMETS, C., GORDON, R.G. A and ARGUS, D.F., 2010. Geologically current plate motions. *Geophys. Journ. Int.,* **181**, 1-80. https://doi.org/10.1111/j.1365-246X.2009.04491.x

DOLATI, A., 2010. Stratigraphy, structural geology and low-temperature thermochronology across the Makran accretionary wedge in Iran. Ph.D Thesis, ETH Zurich, 309 pp. https://doi.org/10.3929/ETHZ-A-006226348

ELGER, J., BERNDT, C., RÜPKE, L., KRASTEL, S., GROSS, F. and GEISSLER, W.H., 2018. Submarine slope failures due to pipe structure formation. *Nat. Commun.* **9,** 715. https://doi.org/10.1038/s41467-018-03176-1

ELLOUZ-ZIMMERMANN, N., DEVILLE, E., MÜLLER, C., LALLEMANT, S., SUBHANI, A.B. and TABREEZ, A.R., 2007. Impact of Sedimentation on Convergent Margin Tectonics: Example of the Makran Accretionary Prism (Pakistan). In: Lacombe, O., Roure, F., Lavé, J. and Vergés, J. (Eds), Thrust Belts and Foreland Basins. *Frontiers in Earth Sciences,* 327-350. https://doi.org/10.1007/978-3-540-69426-7-17.

ELLOUZ-ZIMMERMANN, N., LALLEMANT, S.J., CASTILLA, R., MOUCHOT, N., LETURMY, P., BATTANI, A., BURET, C.,

CHEREL, L., DESAUBLIAUX, G., DEVILLE, E., FERRAND, J., LÜGCKE, A., MAHIEUX, G., MASCLE, G., MÜHR, P., PIERSON-WICKMANN, A.C., ROBION, P., SCHMITZ, J., DANISH, M., HASANY, S., SHAHZAD, A., and TABREEZ, , A., 2007. Offshore Frontal Part of the Makran Accretionary Prism: The Chamak Survey (Pakistan). In: Lacombe O., Roure F., Lavé J., and Vergés J. (Eds). Thrust Belts and Foreland Basins. *Frontiers in Earth Sciences*, Springer. Berlin, Heidelberg. https://doi.org/10.1007/978-3-540-69426-7_18.

ESAN, A.O., 2004. High resolution sequence stratigraphic and reservoir characterization studies of D-07, D-08 and E-01 sands, Block 2 Meren field, offshore Niger Delta. Texas A&M University. Masters Thesis, pp 1-88.

GRANDO, G. and McCLAY, K., 2007. Morphotectonics domains and structural styles in the Makran accretionary prism, offshore Iran. *Sediment. Geol.,* **196**, 157-179. https://doi.org/10.1016/j.sedgeo.2006.05.030

GRIGSBY, J.D., KASSI, A.M. and KHAN, A.S. 2009. Diagenesis of the Oligocene-Early Miocene Panjgur Formation, Paleocene Ispikan Formation and Wakai Exotic Blocks in the Makran Accretionary Belt, Southwest Pakistan. *AAPG Search and Discovery* Article 50143 1-40

HARMS, J.C., CAPPEL, H.N. and FRANCIS, D.C., 1984. The Makran coast of Pakistan: Its stratigraphy and hydrocarbon potential. In: Haq, B.U. and Milliman, J.D. (Eds), Marine Geology and Oceanography of Arabian Sea and Coastal Pakistan. Van Nostrand Reinhold Co., pp 3-26.

HESSLER, A.M. and SHARMAN, G.R., 2018. Subduction zones and their hydrocarbon systems. *Geosphere* **14**, 2044-2067. https://doi.org/10.1130/GES01656.1

HUNTING SURVEY COOPERATION LTD., 1960. Reconnaissance Geology of Part of West Pakistan. Maracle Press, Oshawa, Ontario, Canada, 550 p.

HUSSAIN, A., KHAN, M.R., AHMAD, N. and JAVED, T., 2015. Mud-Diapirism Induced Structuration and Implications for the Definition and Mapping of Hydrocarbon Traps in Makran Accretionary Prism, Pakistan. Society of Exploration Geophysicists and AAPG International Conference & Exhibition, Melbourne, Australia, September 13-16 2015, pp 458-458. https://doi.org/10.1190/ice2015-2194365

KASSI, A.M., GRIGSBY, J.D., KHAN, A.S. and KASI, A. K., 2015. Sandstone petrology and geochemistry of the Oligocene–Early Miocene Panjgur Formation, Makran accretionary wedge, southwest Pakistan: Implications for provenance, weathering and tectonic setting. *Journ. Asian Earth Sci.,* **105**, 192-207. https://doi.org/10.1016/j.jseaes.2015.03.021

KASSI, A.M., KHAN, A.S. and KASI, A. K., 2007. Newly proposed Cretaceous-Palaeocene lithostratigraphy of the Ispikan-Wakai area, southwestern Makran, Pakistan. *Journ. Himal. Earth Sci.,* **40**, 23-31

KASSI, A.M., KHAN, A.S., KELLING, G. and KASI, A.K., 2011. Facies and cyclicity within the Oligocene-Early Miocene Panjgur Formation, Khojak–Panjgur Submarine Fan Complex, south-west Makran, Pakistan. *Journ. Asian Earth Sci.* **41**, 537-550. https://doi.org/10.1016/j.jseaes.2011.03.007

KASSI, A.M., KHAN, S.D., BAYRAKTAR, H. and KASI, A.K., 2014. Newly discovered mud volcanoes in the Coastal Belt of Makran, Pakistan – tectonic implications. *Arab. Journ. Geosci.* **7**, 4899-4909. https://doi.org/10.1007/s12517-013-1135-7

KHAN, I.H. and CLYDE, W.C., 2013. Lower Paleogene Tectonostratigraphy of Balochistan: Evidence for Time-Transgressive Late Paleocene – Early Eocene Uplift. *Geosciences* **3,** 466-501. https://doi.org/10.3390/geosciences3030466

KHAN, M. A., RAZA, H. A. and ALAM, S., 1991. Petroleum Geology of the Makran Region: Implications for Hydrocarbon Occurrence in Cool Basins. *Journal of Petroleum Geology,* **14**, 5-18. https://doi.org/10.1111/j.1747-5457.1991.tb00295.x

KOPP, C., FRUEHN, J., FLUEH, E.R., REICHERT, C., KUKOWSKI, N., BIALAS, J. and KLAESCHEN, D., 2000. Structure of the Makran subduction zone from wide-angle and reflection seismic data. *Tectonophysics* **329**, 171-191. https://doi.org/10.1016/S0040-1951(00)00195-5

LIU, B., CHEN, J., HAIDER, S.W., DENG, X., YANG, L. and DUAN, M., 2020. New high-resolution 2D seismic imaging of fluid escape structures in the Makran subduction zone, Arabian Sea. *China Geol.,* **3**, 269-282. https://doi.org/10.31035/cg2020027

MALKANI, M. S., 2020. Revised Stratigraphy and Mineral Resources of Balochistan Basin, Pakistan: An Update. *Open Journal of Geology,* **10**, 784-828. https://doi.org/10.4236/ojg.2020.107036.

McADOO, B. G., ORANGE, D.L., SCREATON, E., LEE, H.J. and KAYEN, R.E., 2003 Slope basins, headless canyons, and submarine palaeoseismology of the Cascadia accretionary complex. *Basin Research*, **9**(4), 313-324 https://doi.org/10.1046/j.1365-2117.1997.00049.x

McCLAY, K. R., 1990. Deformation mechanics in analogue models of extensional fault systems. In: E. H. Rutter and R. J. Knipe (Eds), Deformation mechanisms, rheology and tectonics. *Geological Society of London Special Publication* **54,** 445-454.

McCLAY, K.R. and ELLIS, P.G., 1987. Geometries of extensional fault systems developed in model experiments. *Geology* **15**, 341-344. doi: https://doi.org/10.1130/0091

MILLER, K.G., KOMINZ, M.A., BROWNING, J.V., WRIGHT, J.D., MOUNTAIN, G.S., KATZ, M.E., SUGARMAN, P.J., CRAMER, B.S., CHRISTIE-BLICK, N. and PEKAR, S.F., 2005. The Phanerozoic record of global sea-level change. *Science*, **310,** 5752, 1293-1298, https://doi.org/10.1126/science.1116412.

MOKHTARI, M., ALA AMJADI, A., MAHSHADINA, L. and RAFIZADEH, M., 2019. A review of the seismotectonics of the Makran Subduction Zone as a baseline for Tsunami Hazard Assessments. *Geosci. Lett.,* **6**, 13. https://doi.org/10.1186/s40562-019-0143-1

NEMATI, M., 2019. Seismotectonic and seismicity of Makran, a bimodal subduction zone, SE Iran. *Journ. Asian Earth Sciences* **169**, 139-164. https://doi.org/10.1016/j.jseaes.2018.08.009

ORI, G. G. and FRIEND, P. F., 1984. Sedimentary basins formed and carried piggyback on active thrust sheets. *Geology* **12** (8), 475-478.

PLATT, J.P., LEGGETT, J.K., YOUNG, J., RAZA, H. and ALAM, S., 1985. Large-scale sediment underplating in the Makran accretionary prism, southwest Pakistan. *Geology* **13**, 507-511. https://doi.org/10.1130/0091-7613(1985)

PLATT, J.P., 1986. Dynamics of orogenic wedges and the uplift of high-pressure metamorphic rocks. *Geol. Soc. Am. Bull.* **97,** 1037-1053.

POSTON, S.W., BERRY, P. and MOLOKWU, F.W., 1983. Meren Field – The Geology and Reservoir Characteristics of a Nigerian Offshore Field. *Journ. Pet. Technol.,* **35,** 2095-2104. https://doi.org/10.2118/10344-PA

REDLINGER, M., BURDICK, J., GREGERSEN, L., RAISHARMA, C. and KROUSKOP, D., 2018. Cook Inlet Natural Gas Availability. *Alaska Division of Oil and Gas,* 1-38. Anchorage, Alaska

SAFARI, A., ABOLGHASEM, A.M., ABEDINI, N. and MOUSAVI, Z., 2017. Assessment of optimum value for dip angle and locking rate parameters in Makran Subduction Zone. *Int. Arch. Photogramm. Remote Sens. Spat. Inf. Sci.* XLII-4/W4, 523-529. https://doi.org/10.5194/isprs-archives-XLII-4-W4-523-2017

SCHLÜTER, H.U., PREXL, A., GAEDICKE, Ch., ROESER, H., REICHERT, CH., MEYER, H. and VON DANIELS, C., 2002a. The Makran accretionary wedge: sediment thicknesses and ages and the origin of mud volcanoes. *Mar. Geol.* **185,** 219-232. https://doi.org/10.1016/S0025-3227(02)00192-5

SMITH, G., McNEILL, L., HENSTOCK, T.J. and BULL, J., 2012. The structure and fault activity of the Makran accretionary prism. *Journ. Geophys. Res. Solid Earth,* **117** B07407. https://

doi.org/10.1029/2012JB0093
STROZYK, F., STRASSER, M., FÖRSTER, A., KOPFT, A. and HUHN, K., 2010. Slope failure repetition in active margin environments: Constraints from submarine landslides in the Hellenic fore arc, eastern Mediterranean. *Journ. Geophys. Res.,* **115**. https://doi:10.1029/2009JB006841
TABREZ, A.R. and INAM, A., 2012 Hydrocarbon Potential in the Makran Offshore Area. *AAPG Search and Discovery* Article 80218, 1-18.
WIEDICKE, M., NEBEN, S. and SPIESS, V., 2001. Mud volcanoes at the front of the Makran accretionary complex, Pakistan. *Marine Geology,* **172**, https://doi.org/10.1016/S0025-3227(00)00127-4
WHITE, R. S. and ROSS, D. A., 1979. Tectonics of the Western Gulf of Oman. *Journ. Geophys. Res.*, **84**, 3479-3489. doi:10.1029/JB084iB07p03479